
MERLIN-ARTHUR CLASSIFIERS: FORMAL INTERPRETABILITY WITH INTERACTIVE BLACK BOXES

Stephan Wäldchen
Zuse Institute Berlin
waelldchen@zib.de

Kartikey Sharma
Zuse Institute Berlin
kartikey.sharma@zib.de

Max Zimmer
Zuse Institute Berlin
zimmer@zib.de

Sebastian Pokutta
Zuse Institute Berlin
pokutta@zib.de

ABSTRACT

We present a new theoretical framework for making black box classifiers such as Neural Networks interpretable, basing our work on clear assumptions and guarantees. In our setting, which is inspired by the Merlin-Arthur protocol from Interactive Proof Systems, two functions cooperate to achieve a classification together: the *prover* selects a small set of features as a certificate and presents it to the *classifier*. Including a second, adversarial prover allows us to connect a game-theoretic equilibrium to information-theoretic guarantees on the exchanged features. We define notions of completeness and soundness that enable us to lower bound the mutual information between features and class. To demonstrate good agreement between theory and practice, we support our framework by providing numerical experiments for Neural Network classifiers, explicitly calculating the mutual information of features with respect to the class.

Keywords XAI · Interpretability · Interactive Proof Systems · Merlin-Arthur Protocol · Mutual Information

1 Introduction

Safe deployment of Neural Network (NN) based AI systems in high-stakes applications, e.g., medical diagnostics [19] or autonomous vehicles [44], requires that their reasoning be subject to human scrutiny. The field of Explainable AI (XAI) has thus put forth a number of interpretability approaches, among them saliency maps [36] and mechanistic interpretability [38]. These have had some successes, such as detecting biases in established datasets [26], or connecting individual neurons to understandable features [9]. However, they are motivated purely by heuristics and come without any theoretical guarantees. Thus, their success cannot be verified and it has been demonstrated for numerous XAI-methods that they can be manipulated by a clever design of the NN [48, 47, 5, 12, 13, 18]. On the other hand, formal approaches to interpretability run into complexity problems when applied to neural networks and require an exponential amount of time to guarantee useful properties [31, 20]. This makes any “right to explanation,” as codified in the EU’s *General Data Protection Regulation* [17], unenforceable.

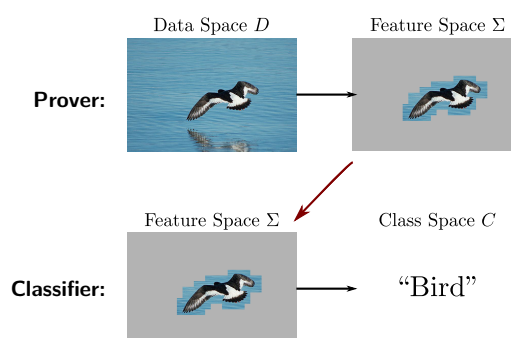


Figure 1: Interactive classification: The prover selects a feature as certificate from the data point and sends it to the classifier. The classifier bases its decision on the provided feature.

In this work, we take a step to overcome both shortcomings by introducing a framework that guarantees feature-based interpretability with legible assumptions. For this, we connect a classification task to the

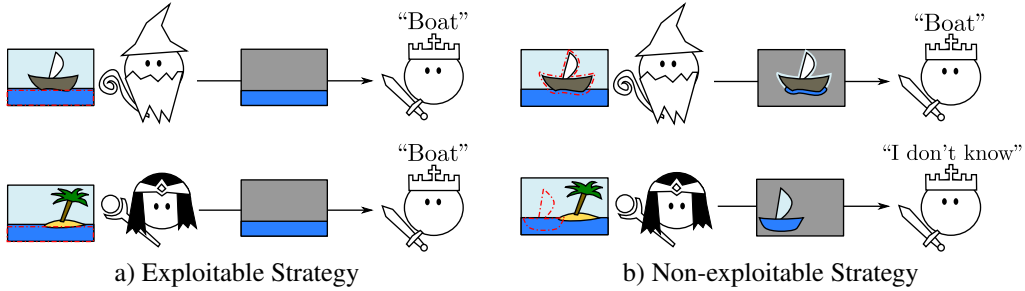


Figure 2: Merlin-Arthur Classification. a) Merlin and Arthur exchange a water feature that is not indicative of the class “Boat”. Morgana can exploit this by selecting the feature for images from a different class causing Arthur to misclassify. b) Merlin and Arthur exchange a feature indicative of the boat class. Arthur insists on the border around the object and Morgana is unable to produce this feature from images without boats.

concept of interactive proof systems (IPS) from computational complexity theory, specifically the Merlin-Arthur protocol [6]. We comment in Section 5 on how our framework can be used to audit commercial classifiers for a “right to explanation”.

For ease of notation, we split the untrustworthy Merlin into a cooperating Merlin and an adversarial Morgana, see Figure 2. Merlin tries to convince Arthur of the correct classification, while Morgana aims for Arthur to give the wrong class. Arthur does not know whether the image comes from Merlin or Morgana. He is allowed to say “I don’t know” if he cannot discern the class, but should not give a wrong answer. For an image from Morgana, this outcome corresponds to the *soundness* criterion, while a correct classification on an image from Merlin improves the *completeness*. It turns out, as we will prove, that the only non-exploitable strategy for Arthur and Merlin is to exchange features that are indeed highly indicative of the true class label with respect to the data distribution. The criteria of completeness and soundness provide guarantees for the explanation, without the need to model the data distribution explicitly. The intuition for this is as follows: If Merlin and Arthur agree to use a feature ϕ for class l which is not indicative of l , then Morgana can select ϕ in an image of a different class than l (as ϕ is not indicative) to fool Arthur into giving the incorrect label. Training Arthur against Morgana can be seen as a type of *robustness*, similar to adversarial robustness [49].

Contribution We develop a novel framework for interactive classification. To evaluate a feature-based XAI-approach one needs to quantify the information content of the features which requires a trustable model of the data manifold [16, 51]. This is difficult to obtain and verify. In our setup we circumvent this by introducing notions of *completeness* and *soundness*, similar to those used in IPS, that can be measured empirically on datasets. Using them we derive bounds on the mutual information of the features with respect to the class without requiring a model of the data manifold. We extend our theorems to actors of bounded computational power and possibly biased datasets.

For the numerical investigation, we model Arthur as a NN. Merlin and Morgana are either non-convex optimisers that solve for the optimal features or trained UNets which predict a feature mask. The MNIST dataset is simple enough that for small features we can find multiple images containing them. This allows us to estimate the mutual information of a feature with respect to the class via sampling. We demonstrate that without Morgana, Arthur and Merlin can “cheat” by communicating via the mask instead of the feature. This demonstration cautions us to re-evaluate self-interpreting setups and optimiser based approaches without guarantees. The “cheating” can be avoided when Morgana is present and we show that our theoretical bounds correspond well to the experimental results. As a sanity check, we compare our setup to other saliency methods and see that they give similar results.

We thus connect notions of robustness to interpretability, a game theoretic equilibrium to mutual information, and interactive proofs to applied machine learning.

Related Work Prime Implicant Explanations [46], a concept from logical abduction, can be efficiently computed for simple classifiers like decision trees [22] and monotonic functions [33]. This concept has been extended to NNs [20], however, it has been shown that approximating small implicants within any non-trivial factor is NP-hard [50] for networks of two layers or more. In [8], the authors construct an algorithm that circumvents these hardness results by further relaxation of the problem. While this is a noteworthy theoretical result, the polynomial bound on the feature size grows so quickly compared to the dimension of the data space that the algorithm does not guarantee useful features for real-world data.

On a different note, there has been impressive progress in designing self-explaining NNs. Networks based on concept encoders [4, 32] or the information bottleneck [2, 7] are motivated by sound ideas and produce

features that are judged well by humans. Yet so far, both approaches are heuristics without guarantees on the quality of the produced explanations.

The work closest in spirit to our setup is AI safety via debate [21]. In their paper, the authors aim to enhance the capabilities of a classifier by selecting features using a “debate” carried out via an interactive game system. They illustrate their method on the MNIST dataset using agents modelled by Monte Carlo Tree Search. The key distinction between the “debate” method and our work is that in [21] Arthur has simultaneous access to the features of both provers, whereas in our case he evaluates them individually. We show in Appendix A.3 that this difference is crucial to derive theoretical results of the same generality as ours. Combining the two approaches to generate guarantees on higher-level interpretations could be a fruitful area of research.

2 Theoretical Framework

What reasonably constitutes a feature strongly depends on the context. In images, it might make sense to regard translations or rotations of a subset of pixels as essentially the same feature or to restrict oneself to connected subsets of pixels up to certain size. We thus opt to leave the definition of a feature completely abstract and define a feature as the set of data points that contain it.

Definition 2.1 (Feature Space). *Given a dataset D , we call a set $\Sigma \subseteq 2^D$ a feature space on D if*

1. $\cup \Sigma = D$, i.e., all data points have at least one feature,
2. $\emptyset \in \Sigma$, i.e., the empty set is contained as a default feature that appears in no data point,
3. For $\mathbf{x}, \mathbf{y} \in D : \mathbf{x} \neq \mathbf{y} \Rightarrow \exists \phi \in \Sigma : (\mathbf{x} \in \phi \wedge \mathbf{y} \notin \phi) \vee (\mathbf{x} \notin \phi \wedge \mathbf{y} \in \phi)$, i.e., two different datapoints are discernible by at least one feature,
4. $\max_{\mathbf{x} \in D} |\{\phi \in \Sigma \mid \mathbf{x} \in \phi\}| < \infty$, i.e., there are only finitely many features per data point.

We say a data point \mathbf{x} contains a feature $\phi \in \Sigma$ if $\mathbf{x} \in \phi$. We also say that a set of features $F \subset \Sigma$ covers the data points in $\bigcup_{\phi \in F} \phi$ which we abbreviate as $\cup F$.

One important practical example of a feature space is given in Example 2.2. Every feature corresponds to a subset of pixels S of size k in an image \mathbf{x} , and any data point \mathbf{y} that has the same values on the subset, i.e., $\mathbf{y}_S = \mathbf{x}_S$, contains the same feature.

Example 2.2 (Features as partial vectors of size k). *Let $D \subset [0, 1]^d$. For $k \in [d]$ we define a feature space corresponding to partial vectors with support of size k subsets as*

$$\Sigma = \bigcup_{\mathbf{x} \in D} \bigcup_{S \subset [d], |S|=k} \{ \{ \mathbf{y} \in D \mid \mathbf{y}_S = \mathbf{x}_S \} \} \cup \{ \emptyset \}.$$

We now define a data space. For notational simplicity, we restrict ourselves to two classes.

Definition 2.3 (Two-class Data Space). *We call the tuple $\mathcal{D} = ((D, \sigma, \mathcal{D}), c, \Sigma)$ a two-class data space if*

1. $D \subseteq [0, 1]^d$ with $d \in \mathbb{N}$ is the set of possible data points,
2. σ is a σ -Algebra on D ,
3. $\mathcal{D} : \sigma \rightarrow [0, 1]$ is a probability measure on D representing the data distribution,
4. $c : D \rightarrow \{-1, 1\}$ is the true classification function,
5. Σ is a feature space on D .

The class imbalance B of a two-class data space is $\max_{l \in \{-1, 1\}} \mathbb{P}_{\mathbf{x} \sim \mu}[c(\mathbf{x}) = l] / \mathbb{P}_{\mathbf{x} \sim \mu}[c(\mathbf{x}) = -l]$.

We now introduce the notion of a feature selector as the prover in our setup.

Definition 2.4 (Feature Selector). *For a given dataset D , we call M a feature selector, if*

$$M : D \rightarrow \Sigma \quad \text{s.t.} \quad \forall \mathbf{x} \in D : (\mathbf{x} \in M(\mathbf{x})) \vee (M(\mathbf{x}) = \emptyset),$$

which means that for every data point $\mathbf{x} \in D$ the feature selector M selects a feature that is present in it or returns the empty set. We call $\mathcal{M}(D)$ the space of all feature selectors for a dataset D .

Definition 2.5 (Partial Classifier). *We define a partial classifier for a feature space Σ as a function $A : \Sigma \rightarrow \{-1, 0, 1\}$. Here, 0 corresponds to the situation where the classifier is unable to identify a correct class. We call the space of all partial classifiers \mathcal{A} .*

2.1 Information Measures: Conditional Entropy and Average Precision

When can we say that a feature truly carries the class information? Surely, a relevant feature should have maximal mutual information with the class. For a given feature $\phi \in \Sigma$ and a data point $\mathbf{y} \sim \mathcal{D}$ the mutual information is defined as

$$I_{\mathbf{y} \sim \mathcal{D}}(c(\mathbf{y}); \mathbf{y} \in \phi) := H_{\mathbf{y} \sim \mathcal{D}}(c(\mathbf{y})) - H_{\mathbf{y} \sim \mathcal{D}}(c(\mathbf{y}) \mid \mathbf{y} \in \phi).$$

When the conditional entropy $H_{\mathbf{y} \sim \mathcal{D}}(c(\mathbf{y}) | \mathbf{y} \in \phi)$ goes to zero, the mutual information becomes maximal and reaches the pure class entropy $H_{\mathbf{y} \sim \mathcal{D}}(c(\mathbf{y}))$ which measures how uncertain we are about the class a priori. A closely related concept is the *precision*. Given a data point \mathbf{x} with feature ϕ , the precision is defined as $\mathbb{P}_{\mathbf{y} \sim \mathcal{D}}[c(\mathbf{y}) = c(\mathbf{x}) | \mathbf{y} \in \phi]$ and was introduced in the context of interpretability [41, 37]. The precision can be used to bound the conditional entropy and thus the mutual information. We now extend this definition to a feature selector.

Definition 2.6 (Average Precision). *For a given two-class data space $((D, \sigma, \mathcal{D}), c, \Sigma)$ and a feature selector $M \in \mathcal{M}(D)$, we define the average precision of M with respect to \mathcal{D} as*

$$Q_{\mathcal{D}}(M) := \mathbb{E}_{\mathbf{x} \sim \mathcal{D}}[\mathbb{P}_{\mathbf{y} \sim \mathcal{D}}[c(\mathbf{y}) = c(\mathbf{x}) | \mathbf{y} \in M(\mathbf{x})]].$$

The average precision $Q_{\mathcal{D}}(M)$ can be used to bound the *average* conditional entropy, defined as

$$H_{\mathbf{x}, \mathbf{y} \sim \mathcal{D}}(c(\mathbf{y}) | \mathbf{y} \in M(\mathbf{x})) := \mathbb{E}_{\mathbf{x} \sim \mathcal{D}}[H_{\mathbf{y} \sim \mathcal{D}}(c(\mathbf{y}) | \mathbf{y} \in M(\mathbf{x}))],$$

and accordingly the average mutual information. For greater detail see Appendix B. We can connect $Q_{\mathcal{D}}(M)$ to the precision of any feature selected by M in the following way.

Lemma 2.7. *Given $\mathfrak{D} = ((D, \sigma, \mathcal{D}), c, \Sigma)$, a feature selector $M \in \mathcal{M}(D)$ and $\delta \in [0, 1]$. Let $\mathbf{x} \sim \mathcal{D}$, then with probability $1 - \delta^{-1}(1 - Q_{\mathcal{D}}(M))$, $M(\mathbf{x})$ selects a feature ϕ , s.t.*

$$\mathbb{P}_{\mathbf{y} \sim \mathcal{D}}[c(\mathbf{y}) = c(\mathbf{x}) | \mathbf{y} \in \phi] \geq 1 - \delta.$$

The proof follows directly from Markov's inequality, see Appendix B. We will now introduce a new framework that will allow us to prove bounds on $Q_{\mathcal{D}}(M)$ and thus assure feature quality. For I and H we will leave the dependence on the distribution implicit when it is clear from context.

2.2 Merlin-Arthur Classification

For a partial classifier A (Arthur) and two feature selectors M (Merlin) and \widehat{M} (Morgana) we define

$$E_{M, \widehat{M}, A} := \left\{ x \in D \mid A(M(\mathbf{x})) \neq c(\mathbf{x}) \vee A(\widehat{M}(\mathbf{x})) = -c(\mathbf{x}) \right\}, \quad (1)$$

as the set of data points for which Merlin fails to convince Arthur of the correct class or Morgana is able to trick him into giving the wrong class, in short, the set of points where Arthur fails. We can now state the following theorem connecting a competitive game to the class conditional entropy.

Theorem 2.8. [Min-Max] *Let $M \in \mathcal{M}(D)$ be a feature selector and let*

$$\epsilon_M = \min_{A \in \mathcal{A}} \max_{\widehat{M} \in \mathcal{M}} \mathbb{P}_{\mathbf{x} \sim \mathcal{D}}[\mathbf{x} \in E_{M, \widehat{M}, A}].$$

Then there exists a set $D' \subset D$ with $\mathbb{P}_{\mathbf{x} \sim \mathcal{D}}[\mathbf{x} \in D'] \geq 1 - \epsilon_M$ such that for $\mathcal{D}' = \mathcal{D}|_{D'}$ we have

$$Q_{\mathcal{D}'}(M) = 1 \quad \text{and thus} \quad H_{\mathbf{x}, \mathbf{y} \sim \mathcal{D}'}(c(\mathbf{y}), \mathbf{y} \in M(\mathbf{x})) = 0.$$

The proof is in Appendix B. This theorem states that if Merlin uses a strategy that allows Arthur to classify almost always correctly, i.e., small ϵ_M , then there exists a dataset that covers almost all of the original dataset and on which the class entropy conditioned on the features selected by Merlin is zero.

Theorem 2.8 states its guarantees for a set D' and not the original set D . We would prefer a less convoluted result such as

$$Q_{\mathcal{D}}(M) \geq 1 - \epsilon_M,$$

which bounds the average precision over the whole dataset. However, this is not straightforwardly possible due to a principle we call *asymmetric feature concentration (AFC)*.

AFC describes a possible quirk of datasets, where a set of features is strongly concentrated in a few data points in one class and spread out over almost all data points in another. We give an illustrative example in Figure 3, and state the formal definition in Appendix B. If a data space \mathfrak{D} has a large AFC κ , Merlin can use features that individually appear in both classes (low precision) to indicate the class where they are spread out over almost all points. But Arthur can then be fooled by Morgana in the other class, where these features are concentrated in a few points, thus ensuring a small ϵ_M .

Though it is difficult to calculate the AFC for complex datasets, we show that it can be bounded above by the maximum number of features per data point in D .

Lemma 2.9. *Let $\mathfrak{D} = ((D, \sigma, \mathcal{D}), c, \Sigma)$ be a two-class data space with AFC of κ . Let $K = \max_{\mathbf{x} \in D} |\{\phi \in \Sigma \mid \mathbf{x} \in \phi\}|$ be the maximum number of features per data point. Then*

$$\kappa \leq K.$$



Figure 3: Example of a dataset with large AFC. The “fruit” features are concentrated in one image for class $l = -1$ but spread out over six images for $l = 1$ (vice versa for the “fish” features). Each individual feature is not indicative of the class as it appears exactly once in each class. Nevertheless, Arthur and Merlin can exchange “fruits” to classify “1” and “fish” for “-1”. The only images where this strategy fails or can be exploited by Morgana are the two images on the left. Regarding Theorem 2.8, we get $\epsilon_M = \frac{1}{7}$ and the set D' corresponds to all images with a single feature. Restricted to D' , the features determine the class completely.

We explain further details in Appendix B. The number K depends on the kind of features one considers. If for $s \times s$ images one considers features in the form of $t \times t$ -pixel masks, there is an upper limit of $(s - t + 1)^2$ features per image, where $s, t \in \mathbb{N}, 0 < t \leq s$. However, this is a worst-case bound—it stands to reason that for real-world data the set of learnable features that can be successfully used by Arthur on a test dataset have an AFC close to one.

2.3 Realistic Algorithms

One reasonable critique could be that we have only shifted the problem of approximating the true data distribution to solving a hard optimisation task, namely finding a perfectly playing Morgana. This is correct, however, we want to make following two points:

1. For a biased dataset it is difficult to establish the accuracy of the approximation to the true data manifold. However, for Morgana we can at least theoretically search over all possible features, even though that is computationally expensive.
2. Morgana only has to find features successfully found by Merlin, albeit in a different class. The question is thus how important are the rest of the features in data points of a class to finding a feature that is *not* strongly correlated to this class.

Instead of presupposing Morgana to be an optimal algorithm, we consider the same algorithm as for Merlin but with the opposite goal. Given $\mathbf{x} \in D$ and a partial classifier A we define

$$M^{\text{opt}}(\mathbf{x}, l) := \operatorname{argmax}_{\phi \in \Sigma} l \cdot A(\phi). \quad (2)$$

Here, M^{opt} returns a mask that convinces Arthur of class l if at all possible. Given a fixed Arthur, $M(\mathbf{x}) = M^{\text{opt}}(\mathbf{x}, c(\mathbf{x}))$ and $\widehat{M}(\mathbf{x}) = M^{\text{opt}}(\mathbf{x}, -c(\mathbf{x}))$ represent the best strategy for Merlin and Morgana respectively. We will henceforth consider Merlin and Morgana to be approximation algorithms for M^{opt} . The question is whether for non-optimal (time and space constrained) agents an equilibrium will emerge that is close to the one for optimal agents. In Appendix B, we explicitly define the notion of *context impact* that lower bounds the success of Morgana relative to Merlin for finding the same features and give an example of a worst-case context impact that illustrates this idea. Generally, our results hold when Morgana is computationally at least as powerful as Merlin. Together with the AFC this allows us to state the following theorem.

Theorem 2.10. *Let $\mathcal{D} = ((D, \sigma, \mathcal{D}), c, \Sigma)$ be a two-class data space with AFC of κ and class imbalance B . Let $A \in \mathcal{A}$, M and $\widehat{M} \in \mathcal{M}(D)$ such that \widehat{M} has a context impact of α with respect to A , M and \mathcal{D} . Define*

1. *Completeness:* $\min_{l \in \{-1, 1\}} \mathbb{P}_{\mathbf{x} \sim \mathcal{D}_l} [A(M(\mathbf{x})) = c(\mathbf{x})] \geq 1 - \epsilon_c,$
2. *Soundness:* $\max_{l \in \{-1, 1\}} \mathbb{P}_{\mathbf{x} \sim \mathcal{D}_l} [A(\widehat{M}(\mathbf{x})) = -c(\mathbf{x})] \leq \epsilon_s.$

Then it follows that

$$Q_{\mathcal{D}}(M) \geq 1 - \epsilon_c - \frac{\alpha \kappa \epsilon_s}{1 - \epsilon_c + \alpha \kappa \epsilon_s B^{-1}}.$$

The proof is found in Appendix B. This theorem is directly relevant for our numerical investigation. The core assumption we make when comparing our lower bound with the measured average precision in Section 3 is the following.

Assumption 2.11. *The AFC κ of \mathcal{D} and the context impact α of \widehat{M} with respect to A , M and \mathcal{D} are both $\simeq 1$.*

Both κ and α are difficult to estimate for high-dimensional datasets, but they offer clear guidelines how to think about your dataset and algorithms in terms of interpretability. We numerically evaluate this assumption on MNIST in Section 3.2, which is simple enough to actually calculate $Q_{\mathcal{D}}(M)$.

2.4 Finite and Biased datasets

After considering realistic algorithms we have to consider realistic, finite datasets on which we evaluate the completeness and soundness criteria. Let us introduce two data distributions \mathcal{T} and \mathcal{D} on the same dataset D , where \mathcal{T} is considered the “true” distribution and \mathcal{D} a different, potentially biased, distribution. We define this bias with respect to a specific feature $\phi \in \Sigma$ as

$$d_{\phi}^l(\mathcal{D}, \mathcal{T}) := |\mathbb{P}_{\mathbf{x} \in \mathcal{D}}[c(\mathbf{x}) = l \mid \mathbf{x} \in \phi] - \mathbb{P}_{\mathbf{x} \in \mathcal{T}}[c(\mathbf{x}) = l \mid \mathbf{x} \in \phi]|.$$

Note that $d_{\phi}^1(\mathcal{D}, \mathcal{T}) = d_{\phi}^{-1}(\mathcal{D}, \mathcal{T}) =: d_{\phi}(\mathcal{D}, \mathcal{T})$ and $0 \leq d_{\phi}(\mathcal{D}, \mathcal{T}) \leq 1$. This distance measures if data points containing ϕ are distributed differently to the two classes for the two distributions.

For example, consider as ϕ the water in the boat images of the PASCAL VOC dataset [26]. The feature is a strong predictor for the “boat” class in the test data distribution \mathcal{D} but should not be indicative for the real world distribution which includes images of water without boats and vice versa. We now want to prove that a feature selected by M is either an informative feature or is misrepresented in the test dataset.

Lemma 2.12. *Let \mathcal{D} , k , B , A , M , α , ϵ_c and ϵ_s be defined as in Theorem 2.10. Let \mathcal{T} be the true data distribution on D . Then for $\delta \in [0, 1]$ we have*

$$\mathbb{P}_{\mathbf{y} \sim \mathcal{T}}[c(\mathbf{y}) = c(\mathbf{x}) \mid \mathbf{y} \in M(\mathbf{x})] \geq 1 - \delta - d_{M(\mathbf{x})}(\mathcal{D}, \mathcal{T}),$$

with probability $1 - \frac{1}{\delta} \left(\frac{k\alpha\epsilon_s}{1+k\alpha\epsilon_s B^{-1}-\epsilon_c} + \epsilon_c \right)$ for $\mathbf{x} \sim \mathcal{D}$.

This follows directly from Lemma 2.7, Theorem 2.10, the definition of $d_{\phi}(\mathcal{D}, \mathcal{T})$ and the triangle inequality. This means that if an unintuitive feature was selected in the test dataset, we can pinpoint to where the dataset might be biased. We include a version of our lemma for the case where we have only limited samples of a potentially biased distribution in Appendix B.

Real World Impact If agents with high completeness and soundness can be successfully trained, they can be used as commercial classifiers that allow for reliable auditing, e.g., in the context of hiring decisions. Using past decisions by the Merlin-Arthur classifier as ground truth, an auditor could use their own Morgana and verify if the setting has sufficient soundness. If so, the features by Merlin must be the basis of the hiring decisions. The auditor can then inspect them for protected attributes, e.g., race, gender or attributes that strongly correlate with them [34]. Our framework thus allows for the “right to explanation” [17] to be enforced even for black box classifiers.

3 Numerical Implementation

We now describe how to train the agents Arthur, Merlin, and Morgana in a general n -class interactive learning setting for image data of dimension d , where $n, d \in \mathbb{N}$. Afterwards, we illustrate our results for the MNIST handwritten digits dataset [11].

Arthur is realised as a feed-forward neural network. He returns a probability distribution over his possible answers, so let $A : [0, 1]^d \rightarrow [0, 1]^{(n+1)}$, corresponding to the probabilities of stating a class or “I don’t know”. The provers select a set S of at most k pixels from the image via a *mask* $\mathbf{s} \in B_k^d$, where B_k^d is the space of k -sparse binary vectors of dimension d . A masked image $\mathbf{s} \cdot \mathbf{x}$ has all its pixels outside of S set to a baseline or a random value. We define the Merlin-loss L_M as the usual cross-entropy loss with regards to the correct class, whereas the Morgana-loss $L_{\widehat{M}}$ considers the total probability of either answering the correct class or the “I don’t know” option, so

$$L_M(A, \mathbf{x}, \mathbf{s}) = -\log(A(\mathbf{s} \cdot \mathbf{x})_{c(\mathbf{x})}) \quad \text{and} \quad L_{\widehat{M}}(A, \mathbf{x}, \mathbf{s}) = -\log(A(\mathbf{s} \cdot \mathbf{x})_0 + A(\mathbf{s} \cdot \mathbf{x})_{c(\mathbf{x})}).$$

The total loss for Arthur is then

$$L_{M, \widehat{M}}(A) = \mathbb{E}_{\mathbf{x} \sim D} \left[(1 - \gamma) L_M(A, \mathbf{x}, M(\mathbf{x})) + \gamma L_{\widehat{M}}(A, \mathbf{x}, \widehat{M}(\mathbf{x})) \right],$$

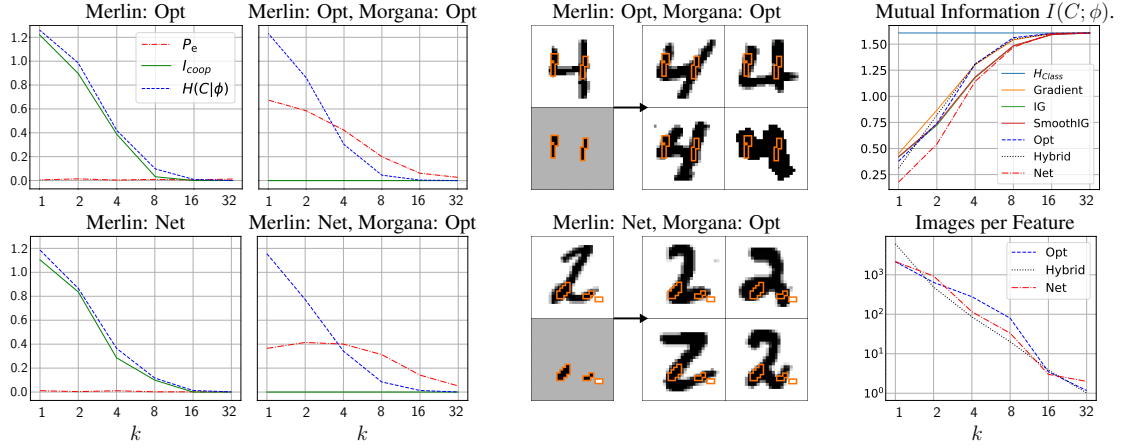


Figure 4: **Left:** “Cheating” measured by I_{coop} over the MNIST test dataset for different setups. In a purely cooperative setup, Arthur and Merlin learn to communicate over uninformative features. Thus, the classification error P_e stays low, while the conditional entropy of the class with respect to the feature goes up. When Morgana is present and soundness is high (in our analysis $\epsilon_s < 0.05$), Arthur and Merlin cannot cheat, the classification error increases for small k . **Middle:** Examples of the feature certificate produced by Merlin for two images. For the “4” feature, there are 13 images in MNIST that share it, all of them of class “4” (we show four here). For the “2” there are 16 images, all of them in “2”. **Right:** As a sanity check, we compare the mutual information at different mask sizes k with established XAI-approaches, see also Appendix C. We also show the average number of images found per feature that we use to estimate the conditional entropy.

where $\gamma \in [0, 1]$ is a tunable parameter. We set $\gamma = 0.75$, since we always want to ensure good soundness. We compare different values of γ in Appendix C. Note that Merlin wants to minimise L_M , whereas Morgana aims to maximise $L_{\widehat{M}}$. In an ideal world, they would solve

$$M(\mathbf{x}) = \operatorname{argmin}_{\mathbf{s} \in B_k^d} L_M(A, \mathbf{x}, \mathbf{s}) \quad \text{and} \quad \widehat{M}(\mathbf{x}) = \operatorname{argmax}_{\mathbf{s} \in B_k^d} L_{\widehat{M}}(A, \mathbf{x}, \mathbf{s}),$$

which we approximate either as optimisers (Frank-Wolfe solver [29]) or as masking networks (U-Net architecture). We kept our training routine simple by basically looping over the three agents, see Algorithm 1. We describe the details of the solvers and architectures in Appendix C.

Algorithm 1 Merlin-Arthur Training

- 1: **Input:** Dataset: D , Epochs: N , γ
 - 2: **Output:** Classifier Network (A), Optional: Masking Networks Merlin (M) and Morgana (\widehat{M})
 - 3: **for** $i \in [N]$ **do**
 - 4: **for** $\mathbf{x}_j, \mathbf{y}_j \in D$ **do**
 - 5: $\mathbf{s}_M \leftarrow M(\mathbf{x}_j, \mathbf{y}_j), \mathbf{s}_{\widehat{M}} \leftarrow \widehat{M}(\mathbf{x}_j, \mathbf{y}_j)$ $\triangleright M$ and \widehat{M} can be the optimiser or the NN
 - 6: $A \leftarrow \operatorname{argmin}_A (1 - \gamma) L_M(A(\mathbf{s}_M \cdot \mathbf{x}_j), \mathbf{y}_j) + \gamma L_{\widehat{M}}(A(\mathbf{s}_{\widehat{M}} \cdot \mathbf{x}_j), \mathbf{y}_j)$ \triangleright Update classifier using masked images
 - 7: $M \leftarrow \operatorname{argmin} L_M(A(M(\mathbf{x}_j) \cdot \mathbf{x}_j), \mathbf{y}_j)$ \triangleright Update only if M is a NN
 - 8: $\widehat{M} \leftarrow \operatorname{argmax} L_{\widehat{M}}(A(\widehat{M}(\mathbf{x}_j) \cdot \mathbf{x}_j), \mathbf{y}_j)$ \triangleright Update only if \widehat{M} is a NN
 - 9: **end for**
 - 10: **for** $\mathbf{x}_j, \mathbf{y}_j \in D$ **do**
 - 11: $A \leftarrow \operatorname{argmin}_A L(A(\mathbf{x}_j), \mathbf{y}_j)$ \triangleright Update classifier using regular images
 - 12: **end for**
 - 13: **end for**
-

3.1 Purely Cooperative Setup and “Cheating”

We first demonstrate that the inclusion of Morgana is necessary for Merlin and Arthur to exchange meaningful features and abstain from “cheating”. For a purely cooperative setup, information about the class $c(\mathbf{x})$ that Arthur infers is dominated by the fact that Merlin chose that feature, rather than the feature itself, i.e., $H(c(\mathbf{x})|M(\mathbf{x}) = \phi) \ll H(c(\mathbf{y})|\mathbf{y} \in \phi)$. We can upper bound $H(c(\mathbf{x})|M(\mathbf{x}) = \phi)$ through the classification error P_e that Arthur and Merlin achieve via Fano’s inequality [14]:

$$H(c(\mathbf{x})|M(\mathbf{x}) = \phi) \leq H_b(P_e) + P_e \log(|C| - 1),$$

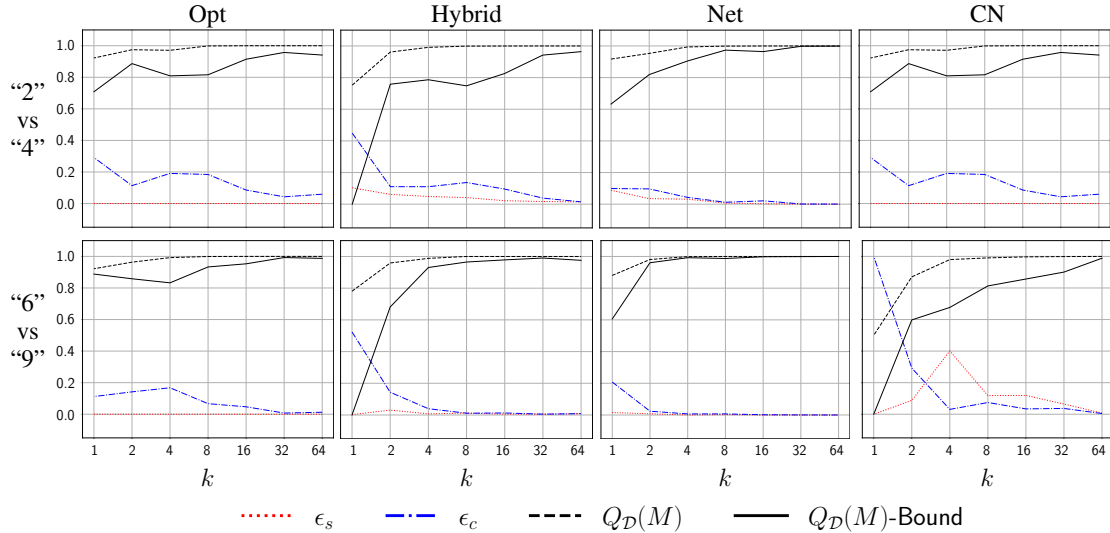


Figure 5: For four different setups of Merlin and Morgana, we compare the lower bound on $Q_{\mathcal{D}}(M)$ with the experimental results on the MNIST dataset. The top row is for the labels $\{“2”, “4”\}$, and the bottom row for $\{“6”, “9”\}$. The bound is tight for large masks but loosens sharply for very small mask sizes k .

where $|C|$ is the number of classes. We can then bound the amount of information that is transferred by the choice of the mask rather than the feature itself as

$$\begin{aligned} I(c(\mathbf{x}); M(\mathbf{x}) = \phi) - I(c(\mathbf{y}); \mathbf{y} \in \phi) &= H(c(\mathbf{y}) | \mathbf{y} \in \phi) - H(c(\mathbf{x}) | M(\mathbf{x}) = \phi) \\ &\geq H(c(\mathbf{y}) | \mathbf{y} \in \phi) - (H_b(P_e) + P_e \log(|C| - 1)), \end{aligned}$$

and for convenience define the *cooperative information* as

$$I_{\text{coop}} := \max(0, H(c(\mathbf{y}) | \mathbf{y} \in \phi) - (H_b(P_e) + P_e \log(|C| - 1))),$$

which lower bounds how much Arthur and Merlin “cheat”. We train Merlin and Arthur on the MNIST dataset and show in Figure 4 that in the purely cooperative case I_{coop} allows keeping the classification error low despite exchanging uninformative features. Including Morgana on the other hand pushes I_{coop} to zero even for small masks. In this case Merlin produces highly informative features, see Figure 4 for two examples.

Why is this observation important? Note that the purely cooperative setup could already be seen as interpretable. With Merlin as a network it appears as a version of a self-interpreting network. With Merlin as an optimiser, it is similar to Rate-Distortion Explanations (RDE) [30]. In fact, RDE have been criticised for producing “cheating” masks that artificially create features that were not present in the original image [51]. We connect this to the lack of robustness with respect to Morgana. Designers of self-interpreting setups need to explain how they circumvent the problem of “cheating” masks.

3.2 Full Setup with Arthur, Merlin and Morgana

To use our theoretical framework we now restrict the MNIST dataset to two classes and train the full Arthur-Merlin-Morgana setup. We measure the completeness and soundness over the test dataset. Theorem 2.10 and Assumption 2.11 allow us to calculate a lower bound on the average precision $Q_{\mathcal{D}}(M)$. We do this once for “2” vs “4” and once for “6” vs “9”, two arbitrary choices. We compare four different setups of feature selectors, one with two Frank-Wolfe optimisers (**Opt**), one where Merlin is a UNet and Morgana an optimiser (**Hybrid**), one where we use UNets for both (**Net**), and one with class-specific networks (**CN**) as explained in Appendix C. In Figure 5 we see that the lower bound is quite tight for larger masks but drops off when k is small. One reason for this is that for very small masks Arthur tends to give up on one of the classes, while keeping the completeness in the other class high. Since the bound considers the minimum over both classes it becomes pessimistic. Regularising Arthur to maintain equal completeness is a potential solution but this is difficult, since this is global information that cannot be easily computed in a single batch.

We see in Figure 5, that when Merlin and Morgana are represented by the same method (both optimisers or NNs), the bound is the tightest. In our hybrid approach, Merlin is at a disadvantage, since he needs to learn a general rule on the training set to select good features, whereas Morgana can optimise directly on the test set during evaluation. It appears the Merlin network is not able to perform as good as an optimiser. In Appendix C we show the same graphs for the training on a larger number of classes. Larger number of

classes generally require larger k to determine the class with the same precision. The training results have greater variance for small masks. This is because there is no optimal strategy for Arthur who cycles between good completeness and soundness.

4 Limitations and Outlook

Our theoretical results are so far only formulated for two classes. We expect them to be extendable to an n -class setting but leave this to further research. It remains to be seen whether our proposed training setup can be extended to more complicated datasets while retaining stability. So far, we have kept the training routine simple and have not explored different training setups. Similar to GAN-training, which is notoriously difficult [43, 52], there is potential for further sophistication.

Features with high mutual information are only a first level interpretation of black box classifiers and do not constitute a full explanation of their decisions. We hope that it is possible to extend our setup to include higher-level reasoning. For example, one can consider multiple Arthurs that are connected by a logical formula such as $f(\mathbf{x}) = A_1(M(\mathbf{x})_1) \vee A_2(M(\mathbf{x})_2)$. In this example, M would be trained to produce two non-overlapping masks. This would allow to find two features that can be considered informative of the class independently. When existing methods highlight different input parts it is usually unclear if they are both necessary or individually sufficient.

5 Conclusion

We provide a new framework inspired by interactive proof systems in which cooperative and adversarial agents achieve a classification together. At equilibrium, this setup becomes interpretable through the exchange of meaningful features, even if the agents individually act as black boxes. We achieve guarantees on the mutual information of the features with respect to the class by expressing it in terms of the average precision and ultimately in terms of measurable criteria such as completeness and soundness. To make required assumptions explicit we introduce the concepts of asymmetric feature correlation and context impact. We extend our results to potentially finite and biased datasets and explain how they can be used to audit commercial classifiers. Finally, we evaluate our results numerically on the MNIST data set. We see that for a purely cooperative setting the exchanged features are uninformative even when the classifier accuracy is high. However, when the setup includes an adversary, we observe high quality features which also demonstrate good agreement between our theoretical bounds and the experimental quality of the exchanged features.

References

- [1] K. Aas, M. Jullum, and A. Løland. Explaining individual predictions when features are dependent: More accurate approximations to shapley values. *arXiv preprint arXiv:1903.10464*, 2019.
- [2] A. Achille and S. Soatto. Information dropout: Learning optimal representations through noisy computation. *IEEE transactions on pattern analysis and machine intelligence*, 40(12):2897–2905, 2018.
- [3] C. Agarwal and A. Nguyen. Explaining image classifiers by removing input features using generative models. In *Proceedings of the Asian Conference on Computer Vision*, 2020.
- [4] D. Alvarez Melis and T. Jaakkola. Towards robust interpretability with self-explaining neural networks. *Advances in neural information processing systems*, 31, 2018.
- [5] C. Anders, P. Pasliev, A.-K. Dombrowski, K.-R. Müller, and P. Kessel. Fairwashing explanations with off-manifold detergent. In *International Conference on Machine Learning*, pages 314–323. PMLR, 2020.
- [6] S. Arora and B. Barak. *Computational complexity: a modern approach*. Cambridge University Press, 2009.
- [7] S. Bang, P. Xie, H. Lee, W. Wu, and E. Xing. Explaining a black-box using deep variational information bottleneck approach. *arXiv preprint arXiv:1902.06918*, 2019.
- [8] G. Blanc, J. Lange, and L.-Y. Tan. Provably efficient, succinct, and precise explanations. *Advances in Neural Information Processing Systems*, 34, 2021.
- [9] S. Carter, Z. Armstrong, L. Schubert, I. Johnson, and C. Olah. Activation atlas. *Distill*, 4(3):e15, 2019.
- [10] C.-H. Chang, E. Creager, A. Goldenberg, and D. Duvenaud. Explaining image classifiers by counterfactual generation. *arXiv preprint arXiv:1807.08024*, 2018.
- [11] L. Deng. The mnist database of handwritten digit images for machine learning research. *IEEE Signal Processing Magazine*, 29(6):141–142, 2012.
- [12] B. Dimanov, U. Bhatt, M. Jamnik, and A. Weller. You shouldn’t trust me: Learning models which conceal unfairness from multiple explanation methods. In *SafeAI@ AAI*, 2020.
- [13] A.-K. Dombrowski, M. Alber, C. J. Anders, M. Ackermann, K.-R. Müller, and P. Kessel. Explanations can be manipulated and geometry is to blame. *arXiv preprint arXiv:1906.07983*, 2019.

- [14] R. M. Fano. Transmission of information: A statistical theory of communications. *American Journal of Physics*, 29(11):793–794, 1961.
- [15] R. C. Fong and A. Vedaldi. Interpretable explanations of black boxes by meaningful perturbation. In *Proceedings of the IEEE international conference on computer vision*, pages 3429–3437, 2017.
- [16] C. Frye, D. de Mijolla, T. Begley, L. Cowton, M. Stanley, and I. Feige. Shapley explainability on the data manifold. *arXiv preprint arXiv:2006.01272*, 2020.
- [17] B. Goodman and S. Flaxman. European union regulations on algorithmic decision-making and a “right to explanation”. *AI magazine*, 38(3):50–57, 2017.
- [18] J. Heo, S. Joo, and T. Moon. Fooling neural network interpretations via adversarial model manipulation. *Advances in Neural Information Processing Systems*, 32:2925–2936, 2019.
- [19] A. Holzinger, C. Biemann, C. S. Pattichis, and D. B. Kell. What do we need to build explainable ai systems for the medical domain? *arXiv preprint arXiv:1712.09923*, 2017.
- [20] A. Ignatiev, N. Narodytska, and J. Marques-Silva. Abduction-based explanations for machine learning models. In *Proceedings of the AAAI Conference on Artificial Intelligence*, volume 33, pages 1511–1519, 2019.
- [21] G. Irving, P. Christiano, and D. Amodei. Ai safety via debate. *arXiv preprint arXiv:1805.00899*, 2018.
- [22] Y. Izza, A. Ignatiev, and J. Marques-Silva. On explaining decision trees. *arXiv preprint arXiv:2010.11034*, 2020.
- [23] M. Jaggi. Revisiting frank-wolfe: Projection-free sparse convex optimization. In *International Conference on Machine Learning*, pages 427–435. PMLR, 2013.
- [24] S. Jain, S. Wiegrefe, Y. Pinter, and B. C. Wallace. Learning to faithfully rationalize by construction. *arXiv preprint arXiv:2005.00115*, 2020.
- [25] J. Kleinberg and E. Tardos. *Algorithm design*. Pearson Education India, 2006.
- [26] S. Lapuschkin, S. Wäldchen, A. Binder, G. Montavon, W. Samek, and K.-R. Müller. Unmasking clever hans predictors and assessing what machines really learn. *Nature communications*, 10(1):1–8, 2019.
- [27] S. Liu, B. Kailkhura, D. Loveland, and Y. Han. Generative counterfactual introspection for explainable deep learning. In *2019 IEEE Global Conference on Signal and Information Processing (GlobalSIP)*, pages 1–5. IEEE, 2019.
- [28] S. M. Lundberg and S.-I. Lee. A unified approach to interpreting model predictions. In *Proceedings of the 31st international conference on neural information processing systems*, pages 4768–4777, 2017.
- [29] J. Macdonald, M. Besancon, and S. Pokutta. Interpretable neural networks with frank-wolfe: Sparse relevance maps and relevance orderings. *arXiv preprint arXiv:2110.08105*, 2021.
- [30] J. Macdonald, S. Wäldchen, S. Hauch, and G. Kutyniok. A rate-distortion framework for explaining neural network decisions. *arXiv preprint arXiv:1905.11092*, 2019.
- [31] J. Macdonald, S. Wäldchen, S. Hauch, and G. Kutyniok. Explaining neural network decisions is hard. In *XXAI Workshop, 37th ICML*, 2020.
- [32] R. Marcinkevičs and J. E. Vogt. Interpretable models for granger causality using self-explaining neural networks. *arXiv preprint arXiv:2101.07600*, 2021.
- [33] J. Marques-Silva, T. Gerspacher, M. C. Cooper, A. Ignatiev, and N. Narodytska. Explanations for monotonic classifiers. In *International Conference on Machine Learning*, pages 7469–7479. PMLR, 2021.
- [34] N. Mehrabi, F. Morstatter, N. Saxena, K. Lerman, and A. Galstyan. A survey on bias and fairness in machine learning. *ACM Computing Surveys (CSUR)*, 54(6):1–35, 2021.
- [35] S. Mertes, T. Huber, K. Weitz, A. Heimerl, and E. André. This is not the texture you are looking for! introducing novel counterfactual explanations for non-experts using generative adversarial learning. *arXiv preprint arXiv:2012.11905*, 2020.
- [36] S. Mohseni, N. Zarei, and E. D. Ragan. A multidisciplinary survey and framework for design and evaluation of explainable ai systems. *ACM Transactions on Interactive Intelligent Systems (TiiS)*, 11(3-4):1–45, 2021.
- [37] N. Narodytska, A. Shrotri, K. S. Meel, A. Ignatiev, and J. Marques-Silva. Assessing heuristic machine learning explanations with model counting. In *International Conference on Theory and Applications of Satisfiability Testing*, pages 267–278. Springer, 2019.
- [38] C. Olah, A. Satyanarayan, I. Johnson, S. Carter, L. Schubert, K. Ye, and A. Mordvintsev. The building blocks of interpretability. *Distill*, 3(3):e10, 2018.
- [39] S. Pokutta, C. Spiegel, and M. Zimmer. Deep neural network training with frank-wolfe. *arXiv preprint arXiv:2010.07243*, 2020.
- [40] D. Rajagopal, V. Balachandran, E. Hovy, and Y. Tsvetkov. Selfexplain: A self-explaining architecture for neural text classifiers. *arXiv preprint arXiv:2103.12279*, 2021.
- [41] M. T. Ribeiro, S. Singh, and C. Guestrin. Anchors: High-precision model-agnostic explanations. In *Proceedings of the AAAI conference on artificial intelligence*, volume 32, 2018.

- [42] O. Ronneberger, P. Fischer, and T. Brox. U-net: Convolutional networks for biomedical image segmentation. In *International Conference on Medical image computing and computer-assisted intervention*, pages 234–241. Springer, 2015.
- [43] K. Roth, A. Lucchi, S. Nowozin, and T. Hofmann. Stabilizing training of generative adversarial networks through regularization. *Advances in neural information processing systems*, 30, 2017.
- [44] J. M. Schraagen, P. Elsasser, H. Fricke, M. Hof, and F. Ragalmuto. Trusting the x in xai: Effects of different types of explanations by a self-driving car on trust, explanation satisfaction and mental models. In *Proceedings of the Human Factors and Ergonomics Society Annual Meeting*, volume 64, pages 339–343. SAGE Publications Sage CA: Los Angeles, CA, 2020.
- [45] L. S. Shapley. *17. A value for n-person games*. Princeton University Press, 2016.
- [46] A. Shih, A. Choi, and A. Darwiche. A symbolic approach to explaining bayesian network classifiers. *arXiv preprint arXiv:1805.03364*, 2018.
- [47] D. Slack, S. Hilgard, E. Jia, S. Singh, and H. Lakkaraju. Fooling lime and shap: Adversarial attacks on post hoc explanation methods. In *Proceedings of the AAAI/ACM Conference on AI, Ethics, and Society*, pages 180–186, 2020.
- [48] D. Slack, S. Hilgard, H. Lakkaraju, and S. Singh. Counterfactual explanations can be manipulated. *arXiv preprint arXiv:2106.02666*, 2021.
- [49] F. Tramer and D. Boneh. Adversarial training and robustness for multiple perturbations. *Advances in Neural Information Processing Systems*, 32, 2019.
- [50] S. Waeldchen, J. Macdonald, S. Hauch, and G. Kutyniok. The computational complexity of understanding binary classifier decisions. *Journal of Artificial Intelligence Research*, 70:351–387, 2021.
- [51] S. Wäldchen, F. Huber, and S. Pokutta. Training characteristic functions with reinforcement learning: Xai-methods play connect four. *arXiv preprint arXiv:2202.11797*, 2022.
- [52] M. Wiatrak, S. V. Albrecht, and A. Nystrom. Stabilizing generative adversarial networks: A survey. *arXiv preprint arXiv:1910.00927*, 2019.
- [53] M. Yu, S. Chang, Y. Zhang, and T. S. Jaakkola. Rethinking cooperative rationalization: Introspective extraction and complement control. *arXiv preprint arXiv:1910.13294*, 2019.

Appendix A Conceptual Overview

As we mentioned in Section 1, finding informative features is a hard computational problem when considering complex classifiers such as neural networks. Efficient algorithms thus cannot be proven to find informative features. An alternative is to measure the informativeness of the features once they have been found by a heuristic algorithm. We will explain in this chapter why this requires a good model of the data distribution, that this is generally a difficult problem as well, and what can go wrong if the data distribution is modelled incorrectly.

Our setup circumvents both problems by linking quantities that are easy to measure, completeness and soundness, to quality bounds on the features exchanged between Merlin and Arthur in an adversarial setup including Morgana. We furthermore illustrate how different self-explaining setups are linked to a purely cooperative setup. Finally, we show with an explicitly constructed data space that the debate setup [21] cannot be used to reproduce our results with the same generality. Instead it would require stronger assumptions on either the classifier or the data space to exclude our counterexample.

A.1 Measuring Feature Importance on the True Data Distribution

We introduce Merlin-Arthur classification so that we can measure the feature quality via the completeness and soundness values over a test dataset. This would not be necessary if we could directly measure the feature quality over the dataset (though it would still be faster than measuring every individual feature). The reason we need the Merlin-Arthur setup is that for general datasets the conditional entropy

$$H_{\mathbf{y} \sim \mathcal{D}}(c(\mathbf{y}) \mid \mathbf{y} \in \phi) = H_{\mathbf{y} \sim \mathcal{D} \mid \mathbf{y} \in \phi}(c(\mathbf{y})),$$

is difficult to measure, since we do not generally know the conditional distribution $\mathcal{D} \mid \mathbf{y} \in \phi$. This measurement is possible for MNIST for small features since the dataset is very simple. However, for more complex data, a feature which is sufficiently large so as to be indicative of the class information will in all likelihood not appear twice in the same dataset. We will now discuss some approaches that aim to approximate the conditional data distribution and what problems they face.

Modelling the conditional data distribution has been pursued in the context of calculating Shapley values, a different interpretability method based on *characteristic functions* from cooperative game theory that assigns a value to every subset of a number of features [45]. We will shortly discuss the approach proposed in [28],

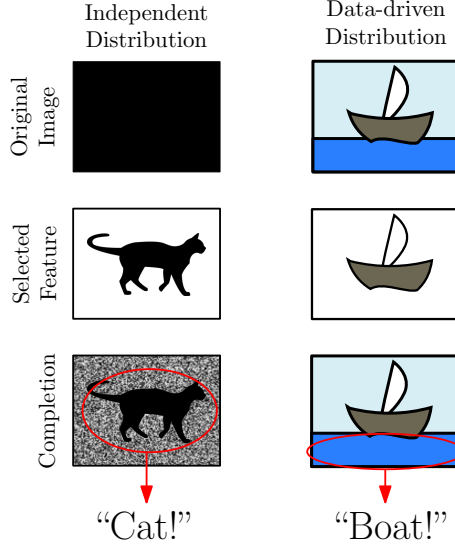


Figure 6: Different failure modes of unrepresentative distributions. *Left*: Independent, random inpainting, similar to [30]. From a black image the shape of a cat is selected and the rest is filled with uniform noise. The shape of a cat is detected by a classifier. *Right*: Data-driven inpainting, similar to [3]. The image of a ship is given and the ship-feature is selected. The data driven distribution inpaints the water back into the image, since in the dataset ships are always on water. The faulty classifier that relies on the water feature is undetected as the ship-feature indirectly leads to the correct classification.

where features correspond to partial vectors supported on sets, see Example 2.2 for how the feature set is defined in that case.

Let $f : [0, 1]^d \rightarrow \{-1, 1\}$ be a classifier function. Then we can naturally define a characteristic function $\nu_{f, \mathbf{x}} : \mathcal{P}([d]) \rightarrow [-1, 1]$ as

$$\nu_{f, \mathbf{x}}(S) = \mathbb{E}_{\mathbf{y} \sim \mathcal{D}}[f(\mathbf{y}) \mid \mathbf{y}_S = \mathbf{x}_S] = \int f(\mathbf{y}_S, \mathbf{x}_{S^c}) d\mathbb{P}_{\mathbf{y} \sim \mathcal{D}}(\mathbf{y}_{S^c} \mid \mathbf{y}_S = \mathbf{x}_S).$$

The Shapley value for input component x_i is then defined as

$$\text{Shapley Value}(x_i) = \frac{1}{d} \sum_{S \subseteq [d] \setminus \{i\}} \binom{d-1}{|S|}^{-1} (\nu_{f, \mathbf{x}}(S \cup \{i\}) - \nu_{f, \mathbf{x}}(S)).$$

In [29] the characteristic function is instead used to define a feature selection method as

$$\mathbf{x}_{S^*} \quad \text{s.t.} \quad S^* = \underset{|S| \leq k}{\operatorname{argmin}} \operatorname{dist}(\nu([d]), \nu(S)),$$

where $k \in [d]$ is a cap on the set size and dist is an appropriate distance measure.

As in our setup the problem is that these approaches depend on how well the conditional probability $\mathbb{P}_{\mathbf{y} \sim \mathcal{D}}(\mathbf{y}_{S^c} \mid \mathbf{y}_S = \mathbf{x}_S)$ is modelled. Modelling the data distribution incorrectly makes it possible to manipulate many existing XAI-methods. This is done by changing the classifier in such a way that it gives the same value on-manifold, but arbitrary value off-manifold. To get feature-based explanations independent of the off-manifold behaviour one needs to model the data manifold very precisely [1, 13]. The authors of [5, 18] and [13] demonstrate this effect for sensitivity analysis, LRP, Grad-Cam, IntegratedGradients and Guided Backprop. They are able to manipulate relevance scores at will and demonstrate how this can be used to obfuscate discrimination inside of a model. LIME and SHAP can be manipulated as well [47] by using a classifier that behaves differently outside off-distribution if the wrong distribution for the explanation. For RDE [30] it is assumed that features are independently and normally distributed, and it was demonstrated that the off-manifold optimisation creates new features that weren't in the original image [51].

We now discuss two approaches proposed to model the data distribution and why each leads to a different problem by under- or over-representing correlation in the data respectively.

Taking an independent distribution: Which means that the conditional probability is modelled as

$$\mathbb{P}_{\mathbf{y} \sim \mathcal{D}}(\mathbf{y}_{S^c} \mid \mathbf{y}_S = \mathbf{x}_S) = \prod_{i \in S^c} p(y_i),$$

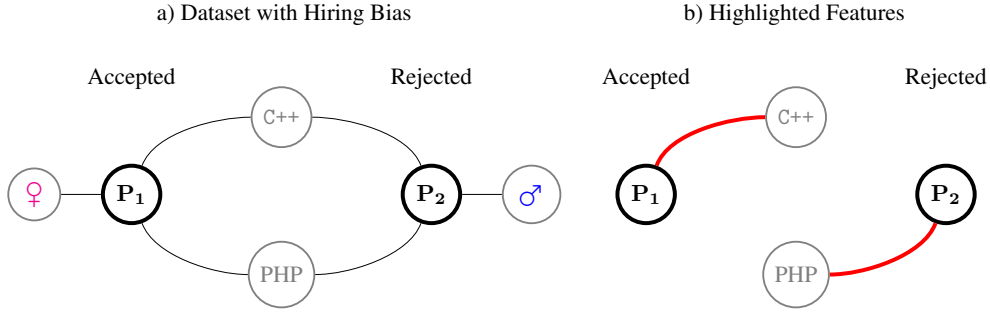


Figure 7: Conceptual illustration of a biased dataset regarding a hiring process and a feature selector that hides this bias. a) Two candidates applied for a position, both are proficient in C++ and PHP and only differ by gender. The female candidate was accepted, while the male candidate was rejected. b) A feature selector highlights one feature for each candidate. In a *faithfulness* test [24], one would retrain a model to reproduce the classification given the selected features to check how much information they carry about the decision. It is clear from this example that the selected features indeed carry this information, not in themselves, but rather through the way they have been selected.

where $p(y_i)$ are suitable probability densities on the individual input components. This approach has been used in [15] and [29], where optimisers are employed to find small features that maximise the classifier score. It was highlighted in [51] how this approach, when modelling the data distribution incorrectly will create artificial new features that were not present in the original image. As we have seen, employing an optimisation method with this distribution can result in “superstimulus” masks— mask that generate new features that weren’t there. We illustrate this problem in Figure 6. Cutting a specific shape out of a monochrome background will with high likelihood result in an image where this shape is visible. If the distribution was true, a monochrome shape would likely lead to an inpainting that is monochrome in the same colour, destroying the artificial feature. But an independent distribution underrepresents these reasonable correlations.

Taking a data-determined distribution via generative model: Which means that the conditional probability is modelled as

$$\mathbb{P}_{\mathbf{y} \sim \mathcal{D}}(\mathbf{y}_{S^c} \mid \mathbf{y}_S = \mathbf{x}_S) = G(\mathbf{y}_{S^c}; \mathbf{x}_S),$$

where G is a suitable generative model. Generative models as a means to approximate the data distribution in the context of explainability have been proposed in a series of publications [3, 10, 27, 35]. This setup introduces a problem. If the network and the generator were trained on the same dataset, the biases learned by the classifier will appear might be learned by the generator as well (see Figure 6 for an illustration)! The important cases will be exactly the kind of cases that we will not be able to detect. If the generator has learned that horses and image source tags are highly correlated, it will inpaint an image source tag when a horse is present. This allows the network to classify correctly, even when the network only looks for the tag and has no idea about horses. The faulty distribution over-represents correlations that are not present in the real-world data distribution.

A.2 Feature Importance and Faithfulness

Recent work has established *faithfulness* as a reasonable criterion (among others) for sound feature selectors and interpretability approaches [24, 40, 53]. Faithfulness is defined as the ability of the model, retrained solely on the selected features for each data point, to infer the correct classification¹. We now want to argue how this approach corresponds to our cooperative setup without Morgana and why one must be careful with the conclusions.

If this retraining should fail, it stands to reason that the selected features were not indicative of the class. However, if the retraining succeeds, it is not necessarily true that the features were also used to make the classification. We already commented on the difference between

$$H(c(\mathbf{x}) \mid M(\mathbf{x}) = \phi) \quad \text{and} \quad H(c(\mathbf{y}) \mid \mathbf{y} \in \phi),$$

in Section 3. The retraining corresponds to our purely cooperative setup in the sense that the model can learn in what pattern the feature selector selects features for each class, without the feature itself being

¹The setup in [53] includes an adversary, however, this adversary operates differently from our Morgana and instead tries to classify on the features *not* selected by Merlin. We have not investigated whether this setup is sufficient to prevent hiding biases as in our example in Figure 7.

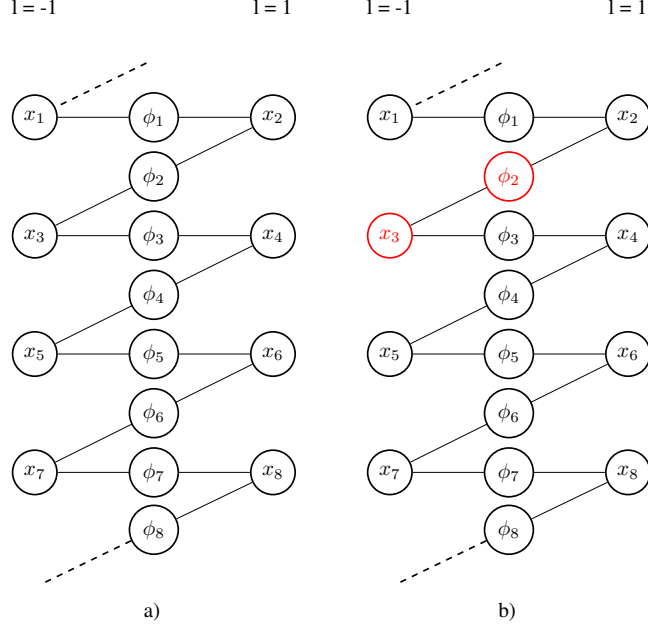


Figure 8: Schematic of \mathcal{D}^{ex} as defined in Example A.1. a) The data space forms a tri-partite graph, where every datapoint shares exactly one feature each with two data points from the opposite class. b) Classification on data point x_3 . Merlin chooses the feature with the smallest index from this data point, so ϕ_2 . Arthur chooses the the class of the datapoint with the highest index compatible with the presented features. Morgana can choose \emptyset , ϕ_2 or ϕ_3 , but in all cases Arthur can correctly identify the original data point and return class $l = -1$.

indicative, see Figure 7 for an illustration, where a feature selector chooses the feature “proficient in C++” for the accepted candidate and “proficient in PHP” for the rejected one even though both have both features. An adversary could easily exploit these uninformative features by reversing the pattern and fooling the classifier into giving the wrong class. This is why robustness with respect to Morgana is necessary to link $H(c(\mathbf{y})|\mathbf{y} \in \phi)$ and $H(c(\mathbf{x})|M(\mathbf{x}) = \phi)$.

A.3 Debate Model vs Merlin-Arthur Classification

The debate setting introduced in [21] is an intriguing alternative to our proposed setup. However, we are now going to present an example data space on which, in debate mode, Arthur and Merlin can cooperate perfectly without using informative features. For this, we use the fact that in the debate setting Arthur receives features from both Merlin and Morgana for each classification. Our example illustrates that the debate setting would need stronger requirements on either the data space or Arthur to produce results similar to ours.

Consider the following Example of a data space \mathcal{D}^{ex} , illustrated in Figure 8.

Example A.1. We define the data space $\mathcal{D}^{\text{ex}} = ((D, \sigma, \mathcal{D}), c, \Sigma)$ with

- $D = \{x_j\}_{j \in [N]}$,
- $\sigma = \mathcal{P}(D)$,
- For $T \in \mathcal{P}(D) : \mathcal{D}(T) = \lfloor \frac{|T|}{N} \rfloor$,
- $c(x_j) = \begin{cases} -1 & j \text{ odd,} \\ 1 & j \text{ even,} \end{cases}$
- $\Sigma = \{\emptyset\} \cup \bigcup_{j \in [N]} \{\phi_j\}$ where $\phi_j = \{x_j, x_{j+1 \bmod N}\}$.

None of the features in Σ are informative of the class, the mutual information $I(c(x); x \in \phi)$ for any $\phi \in \Sigma$ is zero. Nevertheless, in a debate setting Arthur can use the following strategy, when he receives a total of two features from Merlin and Morgana.

$$A(\{\phi_1, \phi_2\}) = \begin{cases} 0 & \text{if } \phi_1 \cap \phi_2 = \emptyset, \\ \max_j c(x_j) \text{ s.t. } x_j \in \phi_1 \cap \phi_2 & \text{otherwise.} \end{cases}$$

which means he returns the class of the data point with the highest j -index that fits the features he is presented (we assume he ignores the \emptyset as a feature). The maximum over the indices should be understood as cyclic, so her prefers N to $N - 1$, but 1 to N , since $N \bmod N = 0$. But now Merlin can use the strategy

$$M(x) = \min_j \phi_j \text{ s.t. } x \in \phi_j,$$

so returning the feature with the lowest j -index. It is easy to check that no matter what Morgana puts forward, the feature with higher or lower index, nothing can convince Arthur of the wrong class. If she gives the same feature as Merlin, the datapoint will be correctly determined by Arthur. If she gives the other feature, the true datapoint is the unique one that has both features. Arthur's strategy works as long as *someone* gives him the feature with the lower index.

In a setting where Arthur has to evaluate every feature individually, the best strategy that Arthur and Merlin can use achieves a $\epsilon_c = \epsilon_s = \frac{1}{3}$, by making use of the asymmetric feature concentration. The AFC for \mathcal{D}^{ex} is $\kappa = 2$, as can be easily checked by taking $F = \{\phi_1, \phi_2, \phi_5, \phi_6\}$ in the definition of the AFC, see Definition B.1, and observing that they cover 4 data points in class $l = -1$ and only two in class $l = 1$. But since the AFC-constant appears in the bound, the lower bound for Q_M is $\frac{1}{6}$, well below the actual average precision of $\frac{1}{2}$.

This example demonstrates that Arthur and Merlin can successfully cooperate even with uninformative features as long as Arthur does not have to classify on features by Morgana alone. This means to produce similar bounds as our setup, the debate mode needs stronger restrictions on either the allowed strategies of Arthur or the structure of the data space, such that this example is excluded.

Appendix B Theoretical Details

We now want to give further explanations to our theoretical investigation in the main part as well as provide definitions and proofs for the theorems and lemmas in the main part.

B.1 Conditional entropy and Average Precision

We now restate the definition of the average precision and average class conditional entropy to show how one can be bound by the other. The average precision of a feature selector M is defined as

$$Q_{\mathcal{D}}(M) := \mathbb{E}_{\mathbf{x} \sim \mathcal{D}}[\mathbb{P}_{\mathbf{y} \sim \mathcal{D}}[c(\mathbf{y}) = c(\mathbf{x}) \mid \mathbf{y} \in M(\mathbf{x})]].$$

The average class conditional entropy with respect to a feature selector is defined as

$$H_{\mathbf{x}, \mathbf{y} \sim \mathcal{D}}(c(\mathbf{y}) \mid \mathbf{y} \in M(\mathbf{x})) := \mathbb{E}_{\mathbf{x} \sim \mathcal{D}}[H_{\mathbf{y} \sim \mathcal{D}}(c(\mathbf{y}) \mid \mathbf{y} \in M(\mathbf{x}))].$$

We can expand the latter and reorder that expression in the following way:

$$\begin{aligned} H_{\mathbf{x}, \mathbf{y} \sim \mathcal{D}}(c(\mathbf{y}) \mid \mathbf{y} \in M(\mathbf{x})) &= -\mathbb{E}_{\mathbf{x} \sim \mathcal{D}} \left[\sum_{l \in \{-1, 1\}} P(c(\mathbf{y}) = l \mid \mathbf{y} \in M(\mathbf{x})) \log(P_{\mathbf{y} \sim \mathcal{D}}(c(\mathbf{y}) = l \mid \mathbf{y} \in M(\mathbf{x}))) \right] \\ &= -\mathbb{E}_{\mathbf{x} \sim \mathcal{D}} \left[\sum_{l \in \{c(\mathbf{x}), -c(\mathbf{x})\}} P(c(\mathbf{y}) = l \mid \mathbf{y} \in M(\mathbf{x})) \log(P_{\mathbf{y} \sim \mathcal{D}}(c(\mathbf{y}) = l \mid \mathbf{y} \in M(\mathbf{x}))) \right] \\ &= \mathbb{E}_{\mathbf{x} \sim \mathcal{D}}[H_b(P_{\mathbf{y} \sim \mathcal{D}}(c(\mathbf{y}) = c(\mathbf{x}) \mid \mathbf{y} \in M(\mathbf{x})))], \end{aligned}$$

where $H_b(p) = -p \log(p) - (1-p) \log(1-p)$ is the binary entropy function. Using that $H_b(p)$ is a concave function together with Jensen's inequality, we can pull in the expectation and arrive at the bound

$$H_{\mathbf{x}, \mathbf{y} \sim \mathcal{D}}(c(\mathbf{y}) \mid \mathbf{y} \in M(\mathbf{x})) \leq H_b(Q_{\mathcal{D}}(M)).$$

We now give a short proof for Lemma 2.7. which we restate here

Lemma 2.7. *Given $\mathcal{D} = ((D, \sigma, \mathcal{D}), c, \Sigma)$, a feature selector $M \in \mathcal{M}(D)$ and $\delta \in [0, 1]$. Let $\mathbf{x} \sim \mathcal{D}$, then with probability $1 - \delta^{-1}(1 - Q_{\mathcal{D}}(M))$, $M(\mathbf{x})$ selects a feature ϕ , s.t.*

$$\mathbb{P}_{\mathbf{y} \sim \mathcal{D}}[c(\mathbf{y}) = c(\mathbf{x}) \mid \mathbf{y} \in \phi] \geq 1 - \delta.$$

Proof. The proof follows directly from Markov's inequality which states that for a nonnegative random variable Z and $\delta > 0$

$$\mathbb{P}[Z \geq \delta] \leq \frac{\mathbb{E}[Z]}{\delta}.$$

Choosing $Z = 1 - \mathbb{P}_{\mathbf{y} \sim \mathcal{D}}[c(\mathbf{y}) = c(\mathbf{x}) \mid \mathbf{y} \in M(\mathbf{x})]$ with $\mathbf{x} \sim \mathcal{D}$ leads to the result. \square

B.2 Min-Max Theorem

We now present the proof for Theorem 2.8 which we restate here.

Theorem 2.8. [Min-Max] Let $M \in \mathcal{M}(D)$ be a feature selector and let

$$\epsilon_M = \min_{A \in \mathcal{A}} \max_{\widehat{M} \in \mathcal{M}} \mathbb{P}_{\mathbf{x} \sim \mathcal{D}} \left[\mathbf{x} \in E_{M, \widehat{M}, A} \right].$$

Then there exists a set $D' \subset D$ with $\mathbb{P}_{\mathbf{x} \sim \mathcal{D}}[\mathbf{x} \in D'] \geq 1 - \epsilon_M$ such that for $\mathcal{D}' = \mathcal{D}|_{D'}$ we have

$$Q_{\mathcal{D}'}(M) = 1 \quad \text{and thus} \quad H_{\mathbf{x}, \mathbf{y} \sim \mathcal{D}'}(c(\mathbf{y}), \mathbf{y} \in M(\mathbf{x})) = 0.$$

Proof. From the definition of ϵ_M it follows that there exists a not necessarily unique $A^\sharp \in \mathcal{A}$ such that

$$\max_{\widehat{M} \in \mathcal{M}} \mathbb{P}_{\mathbf{x} \sim \mathcal{D}} \left[\mathbf{x} \in E_{M, \widehat{M}, A^\sharp} \right] = \epsilon_M. \quad (3)$$

Given A^\sharp , an optimal strategy by Morgana is certainly

$$\widehat{M}^\sharp(\mathbf{x}) = \begin{cases} \phi \text{ s.t. } A(\phi) = -c(\mathbf{x}) & \text{if possible,} \\ \emptyset & \text{otherwise,} \end{cases}$$

and every optimal strategy differs only on a set of measure zero. Thus we can define

$$D' = D \setminus E_{M, \widehat{M}^\sharp, A^\sharp},$$

and have $\mathbb{P}_{\mathbf{x} \sim \mathcal{D}}[\mathbf{x} \in D'] \geq 1 - \epsilon_M$. We know that $A(M(\mathbf{x})) \neq 0$ when $\mathbf{x} \in D'$ and thus can finally assert that

$$\forall \mathbf{x}, \mathbf{y} \in D' : \mathbf{y} \in M(\mathbf{x}) \Rightarrow c(\mathbf{y}) = c(\mathbf{x}),$$

since otherwise there would be at least one $\mathbf{y} \in D'$ that would also be in $E_{M, \widehat{M}^\sharp, A^\sharp}$. Thus we conclude $g_{\mathcal{D}'}(M) = 1$, and from

$$0 \leq H_{\mathcal{D}'}(C, M(X)) \leq H_b(Q_{\mathcal{D}'}(M)) = 0,$$

it follows that $H_{\mathcal{D}'}(C, M(X)) = 0$. \square

This theorem states that if Merlin uses a strategy that allows Arthur to classify almost always correctly, thus small ϵ_M , then there exists a data set that covers almost all of the original data set and on which the class entropy conditioned on the features selected by Merlin is zero.

This statement with a new set D' appears convoluted at first, and we would prefer a simple bound such as

$$Q_{\mathcal{D}}(M) \geq 1 - \epsilon_M,$$

where we take the average precision over the whole data set. This is, however, not straightforwardly possible due to a principle we call *asymmetric feature concentration* and which we introduce in the next section.

B.3 Asymmetric Feature Concentration

Asymmetric feature concentration (AFC) is a concept that will allow us to state our main result. It measures if there is a set of features that are concentrated in a few data points in one class, but spread out over almost all datapoints in the other class. This represents a possible quirk of datasets that can result in a scenario where Arthur and Merlin cooperate successfully with high probability, Morgana is unable to fool Arthur except with low probability—and yet the features exchanged by Arthur and Merlin are uninformative for the class. An illustration of such an unusual data set is given in Figure 9.

For an illustration of the asymmetric feature concentration consider two-class data space $\mathcal{D} = \{(D, \sigma, \mathcal{D}), c, \Sigma\}$, e.g. the “fish and fruit” data depicted in Figure 9. Let us choose $F \subset \Sigma$ to be all the “fish” features. We see that these features are strongly anti-concentrated in class $l = -1$ (none of them share an image) and strongly concentrated in class $l = 1$ (all of them are in the same image).

For now, let us assume F is finite and let $\mathcal{F} = \mathcal{U}(F)$, the uniform measure over F . We have strong AFC if the class-wise ratio of what each feature covers individually is much larger than what the features cover as a whole:

$$\mathbb{E}_{\phi \sim \mathcal{F}} \left[\frac{\mathbb{P}_{\mathbf{x} \sim \mathcal{D}_{-1}}[\mathbf{x} \in \phi]}{\mathbb{P}_{\mathbf{x} \sim \mathcal{D}_1}[\mathbf{x} \in \phi]} \right] \gg \frac{\mathbb{P}_{\mathbf{x} \sim \mathcal{D}_{-1}}[\mathbf{x} \in \cup F]}{\mathbb{P}_{\mathbf{x} \sim \mathcal{D}_1}[\mathbf{x} \in \cup F]}.$$

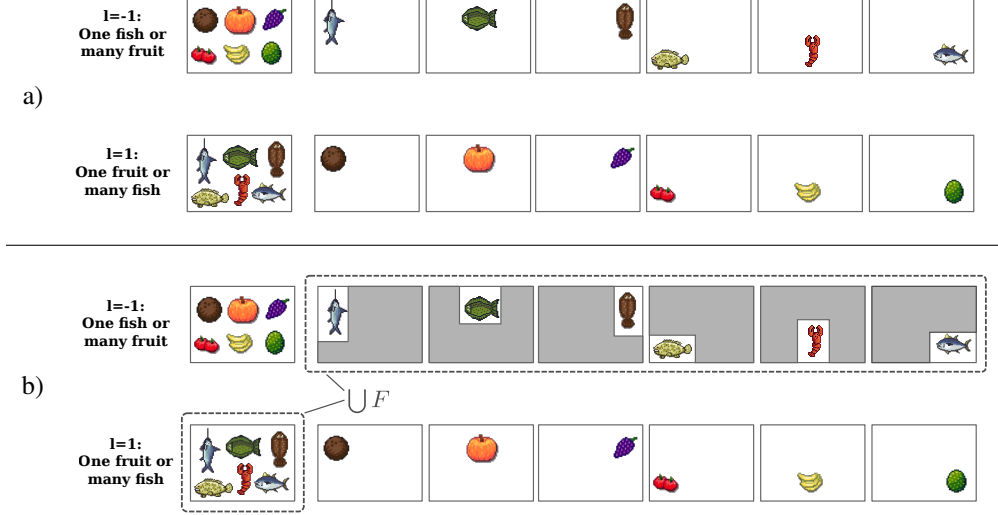


Figure 9: Illustration of a data space with strong asymmetric feature concentration. *a)*: A data set with fish and fruit features. The features are asymmetrically correlated, because all the fruit features are maximally correlated in class -1 (they are all in the same image) and maximally uncorrelated in 1 (no two fruits share the same image). The reverse is true for the fruits. See Figure 10 for a strategy for Merlin that ensures strong completeness and soundness with uninformative features.

b): Asymmetric feature concentration for a specific feature selection. For the class -1 we select the set F of all “fish” features. Each individual fish feature in F covers a fraction of $\frac{1}{6}$ of $(\cup F) \cap D_{-1}$ and all images (one) in $(\cup F) \cap D_1$. The expectation value in Equation (4) thus evaluates to $k = 6$. This is also the maximum AFC for the whole data set as no different feature selection gives a higher value.

In our example, every individual “fish” feature covers one image in each class, so the left side is equal to 1. As a feature set, they cover 6 images in class -1 and one in class 1 , so the right side is $\frac{1}{6}$. Using

$$\frac{\mathbb{P}[\mathbf{x} \in \phi]}{\mathbb{P}[\mathbf{x} \in \cup F]} = \mathbb{P}[\mathbf{x} \in \phi \mid \mathbf{x} \in \cup F],$$

we can restate this expression as

$$\mathbb{E}_{\phi \sim \mathcal{F}}[\kappa_l(\phi, F)] \gg 1, \quad (4)$$

where

$$\kappa_l(\phi, F) = \frac{\mathbb{P}_{\mathbf{x} \sim \mathcal{D}_{-l}}[\mathbf{x} \in \phi \mid \mathbf{x} \in \cup F]}{\mathbb{P}_{\mathbf{x} \sim \mathcal{D}_l}[\mathbf{x} \in \phi \mid \mathbf{x} \in \cup F]}.$$

For our “fish” features we have $\kappa_{-1}(\phi, F) = 6$ for every feature $\phi \in F$. Considering infinite set F , we need a way to get a reasonable measure \mathcal{F} , where we don’t want to “overemphasise” features that appear only in very few data points. We thus define a feature selector $f_F \in \mathcal{M}(\cup F)$ as

$$f_F(\mathbf{x}) = \underset{\substack{\phi \in F \\ \text{s.t. } \mathbf{x} \in \phi}}{\operatorname{argmax}} \kappa(\phi, F), \quad (5)$$

and we can define the push-forward measure $\mathcal{F} = f_{F*} \mathcal{D}_l|_{\cup F}$. For our fish and fruit example, where F is the set of all fish features, f_{F*} would select a fish feature for every image in class -1 that is in $\cup F$. Putting everything together we get the following definition.

Definition B.1 (Asymmetric feature concentration). *Let $((D, \sigma, \mathcal{D}), c, \Sigma)$ be a two-class data space, then the asymmetric feature concentration κ is defined as*

$$\kappa = \max_{l \in \{-1, 1\}} \max_{F \subset \Sigma} \mathbb{E}_{\mathbf{y} \sim \mathcal{D}_l|_{\cup F}} \left[\max_{\substack{\phi \in F \\ \text{s.t. } \mathbf{y} \in \phi}} \frac{\mathbb{P}_{\mathbf{x} \sim \mathcal{D}_{-l}}[\mathbf{x} \in \phi \mid \mathbf{x} \in \cup F]}{\mathbb{P}_{\mathbf{x} \sim \mathcal{D}_l}[\mathbf{x} \in \phi \mid \mathbf{x} \in \cup F]} \right].$$

As we have seen in the “fish and fruit” example, the AFC can be made arbitrarily large, as long as one can fit many individual features into a single image. We can prove that the maximum amount of features per data point indeed also gives an upper bound on the AFC. We now come back to Lemma 2.9 and prove it.

Lemma 2.9. *Let $\mathcal{D} = ((D, \sigma, \mathcal{D}), c, \Sigma)$ be a two-class data space with AFC of κ . Let $K = \max_{\mathbf{x} \in D} |\{\phi \in \Sigma \mid \mathbf{x} \in \phi\}|$ be the maximum number of features per data point. Then*

$$\kappa \leq K.$$

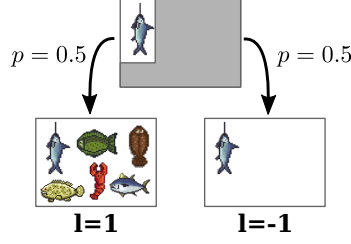


Figure 10: In the data set presented in Figure 9, Merlin can use the strategy to always select the fish features for class $l = -1$ and the fruit features for class $l = 1$ if they exist and choose something arbitrary otherwise. Arthur can then guess $l = 1$ if he gets a fish and $l = -1$ for a fruit. This strategy fails only for the images containing all fruits or fish and can only be exploited by Morgana for those same two images out of 14. The completeness and soundness constants in this case are both $\frac{1}{7}$. But as illustrated here, each “fish” feature is completely uninformative of the class. Conditioned on the selected fish it could either be the image from class $l = -1$ or from $l = 1$.

Proof. Let $l \in \{-1, 1\}$ and let $F \subset \Sigma$. We define $f_F \in \mathcal{M}(UF)$ as in Equation (5) as well as $\mathcal{F} = f_{F^*} \mathcal{D}_l|_{UF}$. We can assert that

$$\mathbb{P}_{\mathbf{x} \sim \mathcal{D}_l}[\mathbf{x} \in \phi \mid \mathbf{x} \in UF] \geq \mathbb{P}_{\mathbf{x} \sim \mathcal{D}_l}[f(\mathbf{x}) = \phi \mid \mathbf{x} \in UF] = \mathcal{F}(\phi). \quad (6)$$

We then switch the order of taking the expectation value in the definition of the AFC:

$$\begin{aligned} \kappa_l(F) &= \mathbb{E}_{\phi \sim \mathcal{F}} \left[\frac{\mathbb{P}_{\mathbf{x} \sim \mathcal{D}_{-l}}[\mathbf{x} \in F \mid \mathbf{x} \in UF]}{\mathbb{P}_{\mathbf{y} \sim \hat{\mathcal{D}}_l}[\mathbf{y} \in \phi \mid \mathbf{y} \in UF]} \right] \\ &= \mathbb{E}_{\phi \sim \mathcal{F}} \left[\frac{\mathbb{E}_{\mathbf{x} \sim \mathcal{D}_{-l}}[\mathbb{1}(\mathbf{x} \in \phi) \mid \mathbf{x} \in UF]}{\mathbb{P}_{\mathbf{y} \sim \hat{\mathcal{D}}_l}[\mathbf{y} \in \phi \mid \mathbf{y} \in UF]} \right] \\ &= \mathbb{E}_{\mathbf{x} \sim \mathcal{D}_{-l}} \left[\mathbb{E}_{\phi \sim \mathcal{F}} \left[\frac{\mathbb{1}(\mathbf{x} \in \phi)}{\mathbb{P}_{\mathbf{y} \sim \hat{\mathcal{D}}_l}[\mathbf{y} \in \phi \mid \mathbf{y} \in UF]} \right] \mid \mathbf{x} \in UF \right]. \end{aligned}$$

Since there are only finitely many features in a data point we can express the expectation value over a countable sum weighted by the probability of each feature:

$$\begin{aligned} \kappa_l(F) &= \mathbb{E}_{\mathbf{x} \sim \mathcal{D}_{-l}} \left[\sum_{\phi \in F: \mathbf{x} \in F} \left[\frac{\mathcal{F}(\phi)}{\mathbb{P}_{\mathbf{y} \sim \hat{\mathcal{D}}_l}[\mathbf{y} \in \phi \mid \mathbf{y} \in UF]} \right] \mid \mathbf{x} \in UF \right] \\ &\leq \mathbb{E}_{\mathbf{x} \sim \mathcal{D}_{-l}} \left[\sum_{\phi \in F: \mathbf{x} \in F} 1 \mid \mathbf{x} \in UF \right] \\ &\leq \mathbb{E}_{\mathbf{x} \sim \mathcal{D}_{-l}}[K \mid \mathbf{x} \in UF] \\ &= K, \end{aligned}$$

where in the first step we used Equation (6) and the definition of K in the second. Then we see that

$$\kappa = \max_{l \in \{-1, 1\}} \max_{F \subset \Sigma} \kappa_l(F) \leq K.$$

□

The number of features per data point is dependent on which kinds of features we consider. Without limitations this number can be 2^d , i.e. exponentially high. See Figure 11 for an example of exponentially

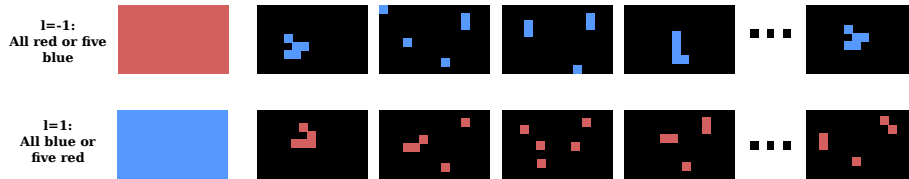


Figure 11: An example of a data set with very high asymmetric feature concentration. The completely red image shares a feature with each of the m -red-pixel images (here $m = 5$), of which there are $\binom{d}{m}$ many. In the worst case $m = \frac{d}{2}$, resulting in $k = \binom{d}{d/2}$ thus exponential growth in d .

large AFC parameter. If we consider, for example for image data, only features of a fixed size and shape the number of features per data point drops to $\approx d$.

We will now prove an intermediate lemma that will later allow us to prove Theorem 2.10.

Lemma B.2. *Let $((D, \sigma, \mathcal{D}), c, \Sigma)$ be a two-class data space with asymmetric feature concentration of κ and class imbalance B . Let $A : [0, 1]^d \rightarrow \{-1, 0, 1\}$ be a partial classifier and $M \in \mathcal{M}(D)$ a feature selector for D . From*

1. *Completeness:*

$$\min_{l \in \{-1, 1\}} \mathbb{P}_{\mathbf{x} \sim \mathcal{D}_l} [A(M(\mathbf{x})) = l] \geq 1 - \epsilon_c,$$

2. *Soundness:*

$$\max_{\widehat{M} \in \mathcal{M}(D)} \max_{l \in \{-1, 1\}} \mathbb{P}_{\mathbf{x} \sim \mathcal{D}_l} [A(\widehat{M}(\mathbf{x})) = -l] \leq \epsilon_s,$$

follows

$$Q_{\mathcal{D}}(M) \geq 1 - \epsilon_c - \frac{\kappa \epsilon_s}{1 - \epsilon_c + \kappa \epsilon_s B^{-1}}.$$

The theorem gives a bound on the probability that data points with features selected by Merlin will also belong to the same class. This probability is large as long as we have a bound on the AFC of the data set.

Proof. The proof of our lemma is fairly intuitive, although the notation can appear cumbersome. Here we give a quick overview over the proof steps.

1. In the definition of the AFC, we maximise over all possible features sets. We will choose as a special case (for each class $l \in \{-1, 1\}$) the features that Merlin selects for data points that Arthur classifies correctly.
2. These feature sets cover the origin class at least up to $1 - \epsilon_c$, and the other class at most up to ϵ_s , which is required by the completeness and soundness criteria respectively. This gives us a high precision for the whole feature set.
3. The AFC upper bounds the quotient of the precision of the whole feature set and expected precision of the individual features, which finally allows us to state our result.

Let us define a partition of D according to the true class and the class assigned by Arthur. From now on let $l \in \{-1, 1\}$ and $m \in \{-1, 0, 1\}$. We introduce the data sets

$$D_{l,m} = \{\mathbf{x} \in D_l \mid A(M(\mathbf{x})) = m\},$$

which means that $D_{l,l}$ are the datapoints that Arthur classifies correctly, and furthermore

$$F_l = M(D_{l,l}).$$

To use the the AFC bound we need a feature selector $f : D_l \cup F_l \rightarrow F$. Merlin itself maps to features outside of F when applied to data points in $D_l \cup F_l \setminus D_{l,l}$. Let us thus define $\sigma : D_l \cup F_l \setminus D_{l,l} \rightarrow F$ which selects an arbitrary feature from F (in case one is concerned whether such a representative can always be chosen, consider a discretised version of the data space which allows for an ordering). Then we can define

$$f(\mathbf{x}) = \begin{cases} M(\mathbf{x}) & \mathbf{x} \in D_{l,l}, \\ \sigma(\mathbf{x}) & \mathbf{x} \in D_l \cup F_l \setminus D_{l,l}, \end{cases} \quad \text{and} \quad F_l = f_* D_l \cup F_l.$$

This feature selector will allow us to use the AFC bound. We now abbreviate

$$p(\mathbf{x}, f) = \mathbb{P}_{\mathbf{y} \sim \mathcal{D}} [c(\mathbf{y}) \neq c(\mathbf{x}) \mid \mathbf{y} \in f(\mathbf{x})] \quad \text{and} \quad P_l = \mathbb{P}_{\mathbf{x} \sim \mathcal{D}} [\mathbf{x} \in D_l].$$

Then

$$1 - Q_{\mathcal{D}}(M) = \mathbb{E}_{\mathbf{x} \sim \mathcal{D}} [p(\mathbf{x}, M)] = \sum_{l \in \{-1, 1\}} \mathbb{E}_{\mathbf{x} \sim \mathcal{D}_l} [p(\mathbf{x}, M)] P_l. \quad (7)$$

Using the completeness criterion and the fact that $p(\mathbf{x}, M) \leq 1$ we can bound

$$\begin{aligned}
\mathbb{E}_{\mathbf{x} \sim \mathcal{D}_l}[p(\mathbf{x}, M)] &= \mathbb{E}_{\mathbf{x} \sim \mathcal{D}_l}[p(\mathbf{x}, M)\mathbb{1}(\mathbf{x} \in D_{l,i})] + \mathbb{E}_{\mathbf{x} \sim \mathcal{D}_l}[p(\mathbf{x}, M)\mathbb{1}(\mathbf{x} \notin D_{l,i})] \\
&\leq \mathbb{E}_{\mathbf{x} \sim \mathcal{D}_l}[p(\mathbf{x}, M)\mathbb{1}(\mathbf{x} \in D_{l,i})] + \epsilon_c \\
&\leq \mathbb{E}_{\mathbf{x} \sim \mathcal{D}_l}[p(\mathbf{x}, M)\mathbb{1}(\mathbf{x} \in D_{l,i})] + \epsilon_c + \mathbb{E}_{\mathbf{x} \sim \mathcal{D}_l}[p(\mathbf{x}, \sigma)\mathbb{1}(\mathbf{x} \in D_l|_{\cup F_l} \setminus D_{l,i})] \\
&\leq \frac{\mathbb{E}_{\mathbf{x} \sim \mathcal{D}_l}[p(\mathbf{x}, M)\mathbb{1}(\mathbf{x} \in D_{l,i}) + p(\mathbf{x}, \sigma)\mathbb{1}(\mathbf{x} \in D_l|_{\cup F_l} \setminus D_{l,i})]}{\mathbb{P}_{\mathbf{x} \sim \mathcal{D}_l}[\mathbf{x} \in D_l|_{\cup F_l}]} + \epsilon_c \\
&= \mathbb{E}_{\mathbf{x} \sim \mathcal{D}_l|_{\cup F_l}}[p(\mathbf{x}, f)] + \epsilon_c \\
&= \mathbb{E}_{\phi \sim \mathcal{F}_l}[\mathbb{P}_{\mathbf{y} \sim \mathcal{D}}[c(\mathbf{y}) = -l | \mathbf{y} \in \phi]] + \epsilon_c.
\end{aligned}$$

We can expand the expression in the expectation using Bayes' Theorem:

$$\begin{aligned}
\mathbb{P}_{\mathbf{y} \sim \mathcal{D}}[c(\mathbf{y}) = -l | \mathbf{y} \in \phi] &= \frac{\mathbb{P}_{\mathbf{y} \sim \mathcal{D}_{-l}}[\mathbf{y} \in \phi]P_{-l}}{\mathbb{P}_{\mathbf{y} \sim \mathcal{D}_{-l}}[\mathbf{y} \in \phi]P_{-l} + \mathbb{P}_{\mathbf{y} \sim \mathcal{D}_l}[\mathbf{y} \in \phi]P_l} \\
&= h\left(\frac{\mathbb{P}_{\mathbf{y} \sim \mathcal{D}_{-l}}[\mathbf{y} \in \phi]P_{-l}}{\mathbb{P}_{\mathbf{y} \sim \mathcal{D}_l}[\mathbf{y} \in \phi]P_l}\right),
\end{aligned}$$

where $h(t) = (1 + t^{-1})^{-1}$. Since $h(t)$ is a concave function for $t \geq 0$, we know that for any random variable R have $\mathbb{E}[h(R)] \leq h(\mathbb{E}[R])$, so

$$\mathbb{E}_{\mathbf{x} \sim \mathcal{D}_l}[p(\mathbf{x}, M)] \leq h\left(\mathbb{E}_{\phi \sim \mathcal{F}_l}\left[\frac{\mathbb{P}_{\mathbf{y} \sim \mathcal{D}_{-l}}[\mathbf{y} \in \phi]}{\mathbb{P}_{\mathbf{y} \sim \mathcal{D}_l}[\mathbf{y} \in \phi]}\right] \frac{P_{-l}}{P_l}\right) + \epsilon_c. \quad (8)$$

From the definition of the AFC κ we know that

$$\mathbb{E}_{\phi \sim \mathcal{F}_l}\left[\frac{\mathbb{P}_{\mathbf{y} \sim \mathcal{D}_{-l}}[\mathbf{y} \in \phi]}{\mathbb{P}_{\mathbf{y} \sim \mathcal{D}_l}[\mathbf{y} \in \phi]}\right] \leq \mathbb{E}_{\mathbf{x} \sim \mathcal{D}_l|_{\cup F_l}}\left[\max_{\substack{\phi \in F \\ \text{s.t. } \mathbf{x} \in \phi}} \frac{\mathbb{P}_{\mathbf{y} \sim \mathcal{D}_{-l}}[\mathbf{y} \in \phi]}{\mathbb{P}_{\mathbf{y} \sim \mathcal{D}_l}[\mathbf{y} \in \phi]}\right] \leq \kappa \frac{\mathbb{P}_{\mathbf{y} \sim \mathcal{D}_{-l}}[\mathbf{y} \in \cup F]}{\mathbb{P}_{\mathbf{y} \sim \mathcal{D}_l}[\mathbf{y} \in \cup F]}. \quad (9)$$

Now we make use of the fact that we can lower bound $\mathbb{P}_{\mathbf{y} \sim \mathcal{D}_l}[\mathbf{y} \in F]$ completeness property

$$\mathbb{P}_{\mathbf{y} \sim \mathcal{D}_l}[\mathbf{y} \in \cup F] \geq 1 - \epsilon_c,$$

and upper bound $\mathbb{P}_{\mathbf{y} \sim \mathcal{D}_{-l}}[\mathbf{y} \in \cup F]$ with the soundness property

$$\mathbb{P}_{\mathbf{y} \sim \mathcal{D}_{-l}}[\mathbf{y} \in \cup F] \leq \epsilon_s,$$

since $\mathbf{y} \in \cup F$ implies that there are features Morgana can use to convince Arthur of class l whereas $\mathbf{y} \sim \mathcal{D}_{-l}$. Together with Equation (8) and Equation (9) we arrive at

$$\mathbb{E}_{\mathbf{x} \sim \mathcal{D}_l}[p(\mathbf{x}, M)] \leq h\left(\kappa \frac{\epsilon_s}{1 - \epsilon_c} \frac{P_{-l}}{P_l}\right) + \epsilon_c = \frac{\kappa \epsilon_s \frac{P_{-l}}{P_l}}{1 - \epsilon_c + \kappa \epsilon_s \frac{P_{-l}}{P_l}} + \epsilon_c.$$

Using $\frac{P_l}{P_{-l}} \leq B$ thus $\frac{P_{-l}}{P_l} \geq B^{-1}$, we can express

$$\mathbb{E}_{\mathbf{x} \sim \mathcal{D}_l}[p(\mathbf{x}, M)] \leq \frac{\kappa \epsilon_s \frac{P_{-l}}{P_l}}{1 - \epsilon_c + \kappa \epsilon_s B^{-1}} + \epsilon_c.$$

Inserted back into equation Equation (7) leads us to

$$1 - Q_{\mathcal{D}}(M) \leq \frac{\kappa \epsilon_s}{1 - \epsilon_c + \kappa \epsilon_s B^{-1}} + \epsilon_c.$$

□

B.4 Context Impact and Realistic Algorithms

As discussed in Section 2.3, Morgana only has to find features that are also findable by Merlin—albeit in images of a different class. The question then becomes how much the other features in the image (the context) matter for finding this feature. We can easily construct scenarios in which the context matters very strongly, see Figure 12 for an example. We expect that for most real-world data this dependence is only weak and can be upper bounded.

Let us make this notion more formal. We want to compare the success rates of Merlin and Morgana conditioned on a convincing feature ϕ with $A(\phi) = l$ being present in the data point:

$$\frac{\mathbb{P}_{\mathbf{x} \sim \mathcal{D}_l}[\widehat{M} \text{ succeeds} | \mathbf{x} \in \phi]}{\mathbb{P}_{\mathbf{x} \sim \mathcal{D}_{-l}}[\widehat{M} \text{ succeeds} | \mathbf{x} \in \phi]}.$$

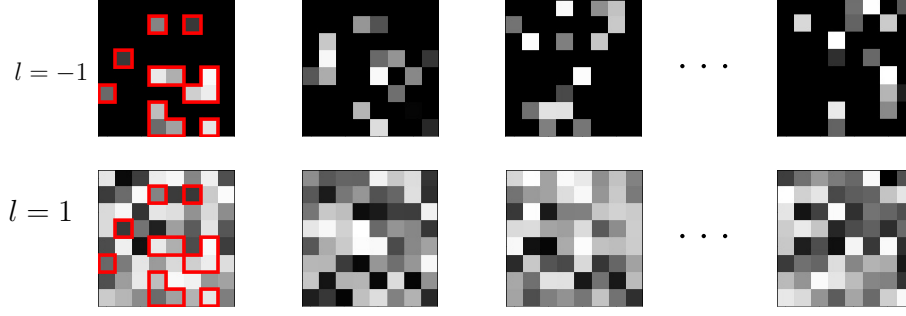


Figure 12: Illustration of a data set with strong context dependence. Class -1 consists of k -sparse images whose pixel values sum to some number S . For each of these images there is a non-sparse image in class 1 that shares all non-zero values (marked in red for the first image). Merlin can use the strategy to show all k non-zero pixels for an image from class -1 and $k + 1$ arbitrary non-zero pixels for class 1. Arthur checks if the sum is equal to S or if the number of pixels equal to $k + 1$, otherwise he says “I don’t know!”. He will then classify with 100% accuracy. Nevertheless, the features Merlin uses for class -1 are completely uncorrelated with the class label. To exploit this, however, Morgana would have to solve the NP-hard[25] subset sum problem to find the pixels for images in class 1 that sum to S . The question is not in which class we can find the features, but in which class we can find the features *efficiently*.

The question is how to define the “success”. If we measure success by returning ϕ , it might be that Morgana can actually find a different feature that convinces Arthur which in that case would not count as a success. If we instead just require that $A(M(\mathbf{x}, l)) = l$ then Merlin could instead rely on a different, easily findable feature that is only present in data points of the correct class. The feature ϕ might then be generally hard to find and Morgana would need to be a again a perfect optimiser. We reason that both approaches would make the fraction unreasonably large even for practical data sets.

The solution is to make the fraction asymmetric and require Merlin to actually find the feature ϕ and Morgana to simply convince Arthur on the data point. So we consider the expression

$$\frac{\mathbb{P}_{\mathbf{x} \sim \mathcal{D}_l} [M(\mathbf{x}) = \phi \mid \mathbf{x} \in \phi]}{\mathbb{P}_{\mathbf{x} \sim \mathcal{D}_{-l}} [A(\widehat{M}(\mathbf{x})) = l \mid \mathbf{x} \in \phi]},$$

and try to assume an upper bound. In the following definition we apply this idea to whole sets of features on which Arthur is constant. That means we maximise over sets $F \subseteq A^{-1}(l)$ where A^{-1} is the preimage of A . If Merlin can find features from this set in one class, then Morgana should not have a much harder time finding them in the other class, given that they are present in the data point.

Definition B.3 (Context Impact). *Let $\mathcal{D} = ((D, \sigma, \mathcal{D}), c, \Sigma)$ be a two-class data space. Let $A \in \mathcal{A}$ and $M: D \times \{-1, 1\} \rightarrow \Sigma^d$ an approximation for M , $\widehat{M} \in \mathcal{M}(D)$. Then the context impact α of \widehat{M} with respect to A , M and \mathcal{D} is defined as*

$$\alpha := \max_{l \in \{-1, 1\}} \max_{F \subseteq A^{-1}(l)} \frac{\mathbb{P}_{\mathbf{x} \sim \mathcal{D}_l} [M(\mathbf{x}) \in F \mid \mathbf{x} \in \cup F]}{\mathbb{P}_{\mathbf{x} \sim \mathcal{D}_{-l}} [A(\widehat{M}(\mathbf{x})) = l \mid \mathbf{x} \in \cup F]}.$$

It might make sense for the definition to require that $\mathcal{D}(\cup F)$ to be large, so that no insignificant feature sets blow up the context dependence, but since we cannot evaluate this quantity numerically anyway we leave this unrestricted for now.

Example B.4. *Let \mathcal{D} be a data space with maximum number of features per datapoint K . Let Morgana operate the algorithm described in Algorithm 2, in which she randomly searches for a convincing feature. Then we have*

$$\alpha \leq \frac{K}{n_{\text{try}}},$$

which corresponds to an upper bound on the probability that Morgana will succeed on an individual datapoint when there is only one convincing feature.

Algorithm 2 Merlin-Arthur Training

- 1: **Input:** $\mathbf{x} \in D$, n_{try}
 - 2: **Output:** $\phi \in \Sigma$
 - 3: **for** $i \in [n_{\text{try}}]$ **do**
 - 4: Pick random feature ϕ s.t. $\mathbf{x} \in \phi$
 - 5: **if** $A(\phi) = -c(\mathbf{x})$ **then**
 - 6: **return** ϕ
 - 7: **end if**
 - 8: **end for**
 - 9: **return** \emptyset
-

We generally want Morgana’s algorithm to be at least as powerful as Merlin’s so in case of an optimiser one can consider giving more iterations or more initial starting values.

We now want to prove Theorem 2.10.

Theorem 2.10. Let $\mathfrak{D} = ((D, \sigma, \mathcal{D}), c, \Sigma)$ be a two-class data space with AFC of κ and class imbalance B . Let $A \in \mathcal{A}$, M and $\widehat{M} \in \mathcal{M}(D)$ such that \widehat{M} has a context impact of α with respect to A , M and \mathfrak{D} . Define

1. *Completeness:* $\min_{l \in \{-1, 1\}} \mathbb{P}_{\mathbf{x} \sim \mathcal{D}_l} [A(M(\mathbf{x})) = c(\mathbf{x})] \geq 1 - \epsilon_c$,
2. *Soundness:* $\max_{l \in \{-1, 1\}} \mathbb{P}_{\mathbf{x} \sim \mathcal{D}_l} [A(\widehat{M}(\mathbf{x})) = -c(\mathbf{x})] \leq \epsilon_s$.

Then it follows that

$$Q_{\mathcal{D}}(M) \geq 1 - \epsilon_c - \frac{\alpha \kappa \epsilon_s}{1 - \epsilon_c + \alpha \kappa \epsilon_s B^{-1}}.$$

Proof. We follow the same proof steps and definitions as in the proof of Lemma B.2 up to Equation (9). Then we consider the following equation

$$\alpha^{-1} \frac{\mathbb{P}_{\mathbf{y} \sim \mathcal{D}_{-l}} [\mathbf{y} \in F]}{\mathbb{P}_{\mathbf{y} \sim \mathcal{D}_l} [\mathbf{y} \in F]} \leq \frac{\mathbb{P}_{\mathbf{y} \sim \mathcal{D}_{-l}} [\mathbf{y} \in F] \mathbb{P}_{\mathbf{x} \sim \mathcal{D}_{-l}} [A(M(\mathbf{x}, l)) = l \mid \mathbf{x} \in F]}{\mathbb{P}_{\mathbf{y} \sim \mathcal{D}_l} [\mathbf{y} \in F] \mathbb{P}_{\mathbf{x} \sim \mathcal{D}_l} [M(\mathbf{x}, l) \in F \mid \mathbf{x} \in F]} \quad (10)$$

$$= \frac{\mathbb{P}_{\mathbf{x} \sim \mathcal{D}_{-l}} [A(M(\mathbf{x}, l)) = l, \mathbf{x} \in F]}{\mathbb{P}_{\mathbf{x} \sim \mathcal{D}_l} [M(\mathbf{x}, l) \in F, \mathbf{x} \in F]} \quad (11)$$

$$= \frac{\mathbb{P}_{\mathbf{x} \sim \mathcal{D}_{-l}} [A(M(\mathbf{x}, l)) = l]}{\mathbb{P}_{\mathbf{x} \sim \mathcal{D}_l} [M(\mathbf{x}, l) \in F]}, \quad (12)$$

where we used in the last step that $M(\mathbf{x}, l) \in F \Rightarrow \mathbf{x} \in F$ and that when $\mathbf{x} \in \mathcal{D}_l$ we have $A(M(\mathbf{x}, l)) = l \Rightarrow \mathbf{x} \in F$ both by definition of F . We know by the soundness criterion

$$\mathbb{P}_{\mathbf{x} \sim \mathcal{D}_{-l}} [A(M(\mathbf{x}, l)) = l] \leq \epsilon_s.$$

From the definition of F and the completeness criterion we get $\mathbb{P}_{\mathbf{x} \sim \mathcal{D}_l} [M(\mathbf{x}, l) \in F] \geq 1 - \epsilon_c$. Putting everything together we arrive at

$$\frac{\mathbb{P}_{\mathbf{y} \sim \mathcal{D}_{-l}} [\mathbf{y} \in F]}{\mathbb{P}_{\mathbf{y} \sim \mathcal{D}_l} [\mathbf{y} \in F]} \leq \frac{\alpha \epsilon_s}{1 - \epsilon_c},$$

which allows us to continue the proof analogously to Lemma B.2. \square

B.5 Finite Data Sets

We provided Lemma 2.12 in the context of biased data sets. The next iteration considers the fact that we only sample a finite amount of data from the possibly biased test data distribution. This will only give us an approximate idea of the soundness and completeness constants.

Lemma B.5. Let $D, \sigma, \mathcal{D}, cA, M$ and \mathcal{T} be defined as in Lemma 2.12. Let $D^{test} = (\mathbf{x}_i)_{i=1}^N \sim \mathcal{D}^N$ be N random samples from \mathcal{D} . Let

$$\epsilon_c^{test} = \max_{l \in \{-1, 1\}} \frac{1}{N} \sum_{\mathbf{x} \in D_l^{test}} \mathbb{1}(A(M(\mathbf{x}, c(\mathbf{x}))) \neq c(\mathbf{x})),$$

and

$$\epsilon_s^{test} = \max_{l \in \{-1, 1\}} \frac{1}{N} \sum_{\mathbf{x} \in D_l^{test}} \mathbb{1}(A(M(\mathbf{x}, -c(\mathbf{x}))) = -c(\mathbf{x})).$$

Then it holds with probability $1 - \eta$ where $\eta \in [0, 1]$ that on the true data distribution \mathcal{T} A and M obey completeness and soundness criteria with

$$\begin{aligned} \epsilon_c &\leq \epsilon_c^{test} + \epsilon_{dist} + \epsilon_{sample} \quad \text{and} \\ \epsilon_s &\leq \epsilon_s^{test} + \epsilon_{dist} + \epsilon_{sample} \end{aligned}$$

respectively, where $\epsilon_{dist} = \max_{l \in \{-1, 1\}} \|\mathcal{D}_l - \mathcal{T}_l\|_{TV}$ and $\epsilon_{sample} = \sqrt{\frac{1}{2N} \log\left(\frac{4}{\eta}\right)}$.

The proof follows trivially from Hoeffding's inequality and the definition of the total variation norm.

Proof. We define $E_{c,l} = \{\mathbf{x} \in D_l \mid A(M(\mathbf{x}, c(\mathbf{x}))) \neq c(\mathbf{x})\}$ for $l \in \{-1, 1\}$ and let $E_{c,l}^{\mathcal{D}}$ be the Bernoulli random variable for the event that $X \in E_{c,l}$ where $X \sim \mathcal{D}$. Then

$$\mathbb{P}_{\mathbf{x} \sim \mathcal{D}_l} [A(M(\mathbf{x}, c(\mathbf{x}))) \neq c(\mathbf{x})] = \mathbb{E}[E_{c,l}^{\mathcal{D}}]$$

Using Hoeffding’s inequality we can bound for any $t > 0$

$$\mathbb{P} \left[\left| \left(\frac{1}{N} \sum_{\mathbf{x} \in D_t^{\text{test}}} \mathbb{1}(\mathbf{x} \in E_{c,l}) \right) - \mathbb{E}[E_{c,l}^{\mathcal{D}}] \right| > t \right] \leq e^{-2nt^2}.$$

We choose t such that $e^{-2t^2} = \frac{\eta}{4}$. We use a union bound for the maximum over $l \in \{-1, 1\}$ which results in a probability of $2 \frac{\eta}{4} = \frac{\eta}{2}$ we have

$$\max_{l \in \{-1, 1\}} \mathbb{E}[E_{c,l}^{\mathcal{D}}] > \epsilon_c^{\text{test}} + \sqrt{\frac{1}{2N} \log\left(\frac{4}{\eta}\right)},$$

and thus with $1 - \frac{\eta}{2}$ we have $\max_{l \in \{-1, 1\}} \mathbb{E}[E_{c,l}^{\mathcal{D}}] \leq \epsilon_c^{\text{test}} + \epsilon^{\text{sample}}$. Using the definition of the total variation norm

$$\|\mathcal{T} - \mathcal{D}\|_{TV} = \sup_{J \subset D} |\mathcal{T}(J) - \mathcal{D}(J)|,$$

with $J = E_{c,l}$ we can derive $\mathbb{E}[E_{c,l}^{\mathcal{T}}] \leq \mathbb{E}[E_{c,l}^{\mathcal{D}}] + \|\mathcal{T} - \mathcal{D}\|_{TV}$ and thus

$$\epsilon_c \leq \epsilon_c^{\text{test}} + \epsilon^{\text{sample}} + \epsilon^{\text{dist}}.$$

We can treat ϵ_s analogously and take a union bound over both the completeness and soundness bounds holding which results in the probability of $1 - \eta$. \square

Appendix C Numerical Experiments

For the numerical experiments, we implement the Arthur, Merlin and Morgana in Python 3.8 using Pytorch (BSD-licensed). We performed our experiments on the MNIST dataset which is licensed under the Creative Commons Attribution-Share Alike 3.0 license. We now give an overview over our training setup and show the error bars of the numerical results presented in the main part of the paper over 10 different training runs.

C.1 Training Setup

Structure of Arthur. Arthur is modelled using a Neural Network. Specifically, we consider a convolutional neural network with a ReLU activation function. For the case of 2 classes, we consider a NN with 2 convolution layers whereas for the 5 class case we consider 3 convolution layers. The output of the convolution is then passed through a 2 linear layers before being used for the output. Table 1 describes the used architecture in detail.

Layer Name	Parameters
Conv2D	I=3, O=32, K=3
ReLU	
Conv2D	I=32, O=64, K=3
ReLU	
Conv2D	I=64, O=64, K=3
ReLU	
MaxPool2d	K=2
Linear	I=7744, O=1024
ReLU	
Linear	I=1024, O=128
ReLU	
Linear	I=128, O=1

Table 1: Description of the neural network architecture used for the Arthur classifier.

Structure of Merlin and Morgana. Recall that Merlin and Morgana aim to ideally solve

$$M(\mathbf{x}) = \operatorname{argmin}_{\mathbf{s} \in B_k^d} L_M(A, \mathbf{x}, \mathbf{s}) \quad \text{and} \quad \widehat{M}(\mathbf{x}) = \operatorname{argmax}_{\mathbf{s} \in B_k^d} L_{\widehat{M}}(A, \mathbf{x}, \mathbf{s}),$$

respectively, where L_M and $L_{\widehat{M}}$ are the loss functions defined in Section 3, and B_k^d is the space of k -sparse binary vectors. Thus Merlin and Morgana take an image as input and produce produce a mask of the same

dimension with k one entries and zero-entries otherwise. We additionally added a regularisation term in the form of

$$\lambda \|s\|_1$$

to both of the objectives, and set $\lambda = 0.25$. We realise Merlin and Morgana in four different ways which we explain in the following. All of these approaches return a mask $s \in [0, 1]^d$ that we then binarise by setting the k largest values to one and the rest to zero.

Frank-Wolfe Optimisers In the first case, Merlin and Morgana are modelled by an optimiser using the Frank-Wolfe algorithm [23]. We follow the approach outlined by [29] with the Frank-Wolfe package provided by [39]. The optimiser searches over a convex relaxation of B_k^d , i.e.,

$$\mathcal{B}_k^d = \{v \in [0, 1]^d \mid \|v\|_1 \leq k\},$$

the k -sparse polytope with radius 1 limited to the positive octant. To optimise the objective we use the solver made available at <https://github.com/ZIB-I0L/StochasticFrankWolfe> with 200 iterations.

UNet Approach For the second case we model Merlin and Morgana using Neural Networks, specifically a UNet. We copy the UNet design by [42] since it achieves good results in image segmentation, a task reasonably similar to ours. We predict mask values between zero and one for each image pixel, and rescale the mask should it lie outside of \mathcal{B}_k^d . The binarisation of the mask is ignored during the backpropagation that trains the UNets and only employed to produce the masks that Arthur is trained on.

Hybrid Approach In the Hybrid approach, Merlin is modelled by a UNet, whereas Morgana is still modelled by the FW-optimiser. This approach is useful since for a sound Arthur that cannot be fooled the training of the Morgana UNet becomes difficult and the UNet diverges. It then takes a while of training for the UNet to adapt, should Arthur open himself to possible adversarial masks. The optimiser is applied to each individual image instead and can find possible weaknesses instantly.

Class-Networks One of the alternatives to Merlin and Morgana that we propose are class-specific UNets. Instead of Merlin and Morgana each being represented by a network, there is a UNet associated with each class that is trained to produce a feature mask that convinces Arthur of its own class for any input image, i.e., for $l \in [C]$ try to solve

$$M_l(\mathbf{x}) = \operatorname{argmin}_{s \in B_k^d} -\log(A(s \cdot \mathbf{x})_l) + \lambda \|s\|_1.$$

Merlin is then implemented as an algorithm to choose the UNet corresponding to the true class, so

$$M(\mathbf{x}) = M_{c(\mathbf{x})}(\mathbf{x}).$$

Morgana instead uses for each individual image the output of the UNet that most convinces Arthur of a wrong class (maximises the Morgana-loss), i.e.

$$M(\mathbf{x}) = M_l(\mathbf{x}) \quad \text{with} \quad l = \operatorname{argmax}_{l \in C \setminus \{c(\mathbf{x})\}} L_{\widehat{M}}(A, \mathbf{x}, M_l(\mathbf{x})).$$

Ideally this training setup would be more stable than the normal UNet approach. When Arthur cannot be fooled, the class-UNets still have a reasonable objective in convincing him of the correct class, which hopefully prevents divergence as for the Morgana UNet. Experimentally however, the class-networks proved to be much less stable than the simple UNet approach, see Figure 1.

We give an overview over the parameters used for the four different approaches in Table 2.

Parameter	Value
Batch Size	128
Baseline Value	0.3
Max FW Iterations	200
FW Momentum	0.9
Regularisation λ	0.25
Max NN Passes	5
Arthur LR	1e-4
Merlin LR	1e-4
Morgana LR	1e-6

Table 2: Values of various parameters used in training.

Merlin-Arthur Classifier Training The overall training procedure proceeds as outlined in Algorithm 1. We initially train Arthur directly on the training data. In the optimiser approach this pre-trained network is used to search for the optimal masks for Merlin and Morgana. In the UNet approach these masks are directly produced by the UNets. Arthur is then trained on the masked images over the whole dataset. The UNets are then trained on the dataset with a fixed Arthur according to their respective objectives. We cycle through this process for 5 epochs. The learning rate is $1e-4$ for the Arthur and Merlin network and $1e-6$ for the Morgana and the class-specific networks.

C.2 Variance over Different Training Runs

Both Figure 13 and Figure 14 depict the results from the main paper in more detail. Specifically, they depict averages and the standard deviation as error bars for each for each parameter using samples from 10 different training runs. We see that, with exception of the class-networks, the results presented here agree with those presented in the main body of the paper. The error bars are large for small mask sizes but shrink as the mask size increases. The class-network approach is considerably less stable than our other implementations, even though it was conceived as a stabler alternative to the simple network approach. One possibility might be that since each UNet both cooperates with Arthur and wants to fool him, they are more sensitive when Arthur changes his focus between achieving good soundness and completeness. We hope that further research will determine if this realisation can be trained in a stable manner.

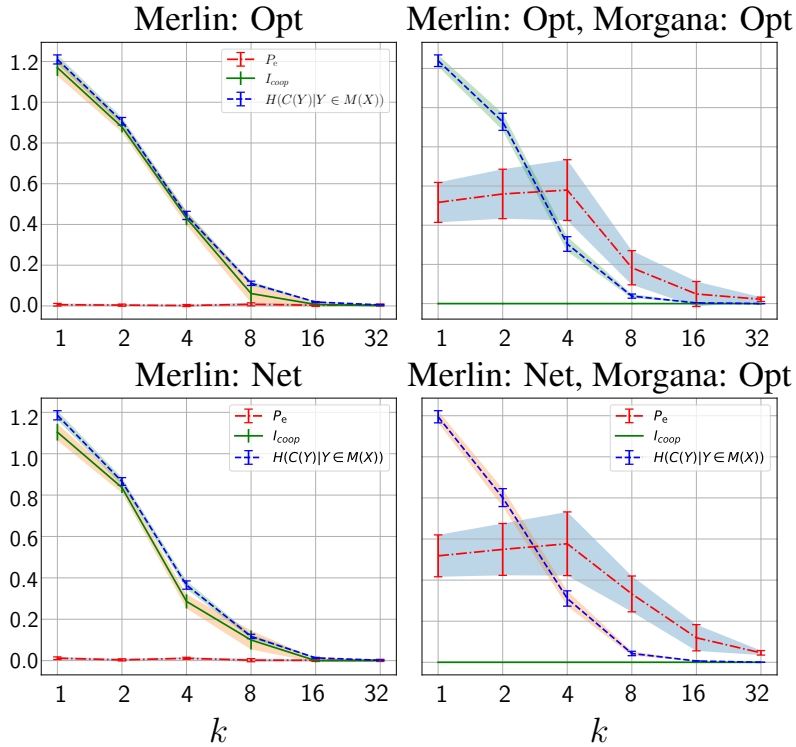


Figure 13: This figure depicts the mean and standard deviation over 10 training runs for the error probability, cooperative information and the class entropy. This was obtained from 5-class classification with classes 1,2,3,4 and 5 with $\gamma = 0.75$ for the purely cooperative setup (*left*) and the adversarial setup (*right*), where Merlin was realised as an optimiser (*top*) or as a neural network (*bottom*).

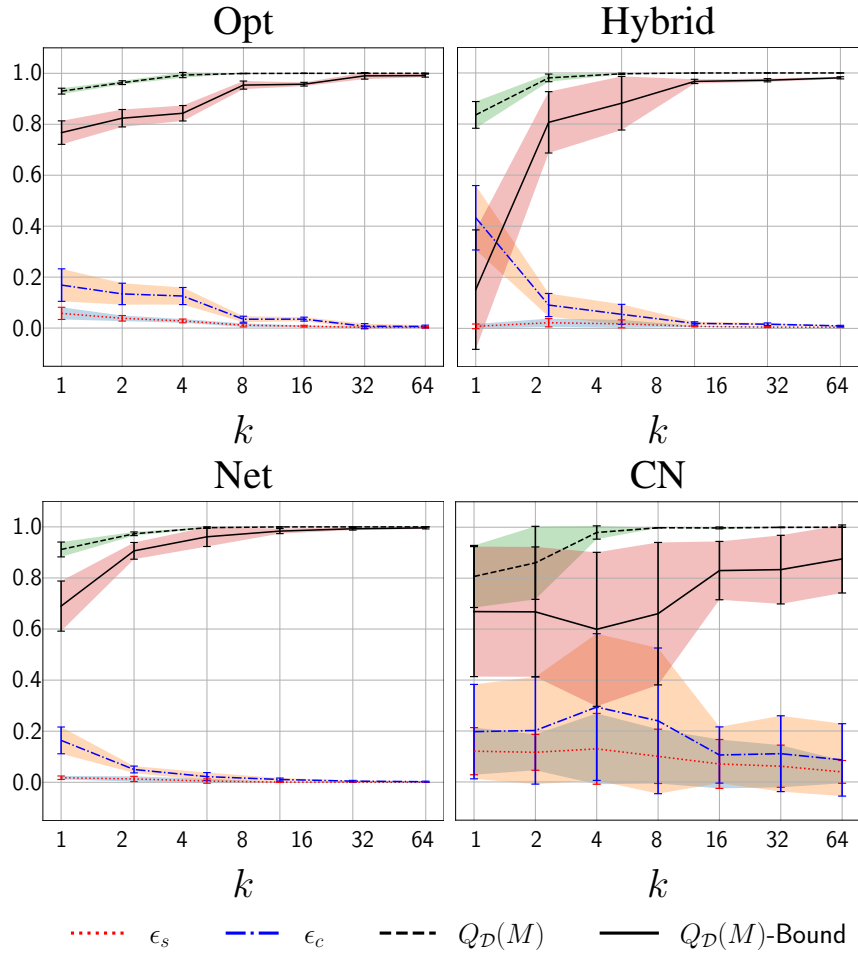


Figure 14: We show the mean and standard deviation over 10 training runs for completeness and soundness, along with the average precision and its bound as obtained from 2-class classification with classes 6 and 9 with $\gamma = 0.75$ for different settings.